

Forschungsprojekt

**Koexistenzoptimierte industrielle
Funksysteme - KOSYS**

Schlussbericht

Zuwendungsempfänger:	Hochschule Ostwestfalen-Lippe - Institut inIT
Förderkennzeichen:	17041X11
Laufzeit des Vorhabens:	01.07.2011 - 31.12.2014

M.Sc. Dimitri Block / Prof. Dr.-Ing. Uwe Meier
Lemgo, 30.06.2015

Projektleitung:

Prof. Dr.-Ing. Uwe Meier
Institut Industrial IT - inIT
Hochschule Ostwestfalen-Lippe
Liebigstrasse 87
D-32657 Lemgo
uwe.meier@hs-owl.de
<http://www.hs-owl.de/fb5>

Projektpartner:

Phoenix Contact Electronics GmbH,
Bad Pyrmont
Weidmüller Interface GmbH & Co. KG,
Detmold
Universität Rostock, Fakultät für Informatik
und Elektrotechnik



Universität
Rostock



Traditio et Innovatio



1 Kurzfassung

Nach zaghaften Anfängen Mitte der 90er Jahre haben sich industrielle Wireless-Technologien zu unverzichtbaren Komponenten der industriellen IT-Infrastruktur entwickelt. Diese Wireless-Systeme zeichnen sich durch den Einsatz unterschiedlicher Funktechnologien aus, weil keine Technologie allen Anforderungen gerecht wird. Dabei werden fast ausschließlich Technologie-Standards verwendet, die auch im Konsumbereich verwendet werden. Die wichtigsten industriell genutzten Standards sind: IEEE 802.11 (WLAN), IEEE 802.15.1 (Bluetooth) und IEEE 802.15.4 (WirelessHART). Bei einem Parallelbetrieb müssen sich diese heterogenen Funktechnologien die Ressourcen Raum, Frequenz und Zeit teilen. Das Koexistenzverhalten ist daher der entscheidende und damit begrenzende Systemparameter. Es hat sich gezeigt, dass das Koexistenzverhalten oft einen stärkeren Einfluss auf die Qualität der Datenübertragung hat als die passiven Effekte des Funkkanals, die durch Mehrwegeausbreitung und Bewegungseffekte hervorgerufen werden.

Im Rahmen dieses Forschungsprojekts wurde erforscht, wie die bekannten Probleme des koexistenzlimitierten Betriebs heterogener Funksysteme in industriellen Einsatzszenarien durch neuartige koexistenzoptimierte Funksysteme auf Basis kognitiver Ansätze vermieden werden können. Koexistenzoptimierte kognitive Funksysteme erreichen in jeder Umgebung stets das optimale Systemverhalten, d.h. eine bestmögliche Qualität der Datenübertragung bei minimaler Störung anderer Funkanwendungen.

Eine erfolgreiche Umsetzung dieser neuen Strategie ermöglicht die folgenden Eigenschaften:

- Bestehende Funksysteme - sogenannte primäre Nutzer - werden durch zusätzliche koexistenzoptimierte kognitive Funksysteme nicht beeinträchtigt.
- Koexistenzoptimierte kognitive Funksysteme erkennen und nutzen bestehende temporale und spektrale Lücken für ihre Datenübertragung als sekundäre Nutzer.
- Die spektrale Effizienz in einem Raumbereich wird durch die zusätzlichen koexistenzoptimierten kognitive Funksysteme verbessert.

Die angestrebten verbesserten Produkteigenschaften industrieller Funksysteme werden letztlich die Akzeptanz funkbasierter Automatisierungskomponenten auf der Anwenderseite verbessern und sich wirtschaftlich auszahlen.

Die wichtigsten Ergebnisse des Projekts sind:

- Die Performance-Grenzen adaptiver und nichtadaptiver Mediumzugriffsverfahren wurden für aktuelle industrielle IEEE 802.1x-Verfahren (WLAN, Bluetooth, WirelessHART) simulativ evaluiert: Während die adaptiven Verfahren Vorteile bezüglich der Paketverlustrate aufweisen, sind die nicht-adaptiven Verfahren bezüglich des Echtzeitverhaltens überlegen. Aber keines dieser Verfahren erfüllt beide Kriterien.
- Das optimale Mediumzugriffsverfahren basiert auf einem kognitiven Ansatz mit einer verteilten spektralen und lokalen temporalen Ressourcenzuweisung. Es wurde experimentell realisiert und evaluiert.

- Die verteilte spektrale Ressourcenzuweisung arbeitet kooperativ wofür ein zentraler Ressourcen-Manager benötigt wird. Das Verfahren ISAC (*inter-system automatic configuration*) wurde hierfür vorgeschlagen. Zusätzlich verwendet es eine breitbandige Funkkanalsensorik mit anschließender Klassifizierung möglicher nicht-kooperierender Störsysteme nach dem NFSC-Prinzip (*neuro-fuzzy signal classifier*).
- Die lokale temporale Ressourcenzuweisung arbeitet autonom mit einem prädiktiven Ansatz. Für schnelle Echtzeitanwendungen hat sich eine energiebasierte Sensorik mit einer Abschätzung der Dauer sowohl der Funkkanalbelegung als auch der Verfügbarkeit basierend auf einer MARKOV-Modellierung mit 4 Übergangszuständen als optimal erwiesen.

Alle Ansätze wurden simulativ bewertet und mittels eines Demonstrators experimentell verifiziert.

2 Inhaltsverzeichnis

1	KURZFASSUNG	3
2	INHALTSVERZEICHNIS.....	5
3	AUFGABENSTELLUNG DES FORSCHUNGSPROJEKTS.....	6
4	VORAUSSETZUNGEN DES FORSCHUNGSPROJEKTS	7
5	PLANUNG UND ABLAUF DES FORSCHUNGSPROJEKTS	8
6	WISSENSCHAFTLICHER UND TECHNISCHER STAND.....	10
7	ZUSAMMENARBEIT MIT ANDEREN STELLEN.....	12
8	ERGEBNISSE DES FORSCHUNGSPROJEKTS – RESULTS OF THE RESEARCH PROJECT	13
8.1	PERFORMANCE EVALUATION OF ADAPTIVE METHODS.....	14
8.1.1	<i>Evaluation Approaches.....</i>	14
8.1.2	<i>Adaptive Methods in Standards</i>	15
8.1.3	<i>Simulative Investigation</i>	17
8.1.4	<i>Performance Evaluation Measures</i>	24
8.1.5	<i>Performance Evaluation Results.....</i>	26
8.2	COEXISTENCE OPTIMIZATION WITH COGNITIVE METHODS	30
8.2.1	<i>Cognitive Methods for Autonomous Medium Access.....</i>	30
8.2.2	<i>Cognitive Methods for Cooperative Medium Access.....</i>	36
8.2.3	<i>Cognitive Methods for Interference Signal Classification.....</i>	39
8.3	PERFORMANCE EVALUATION AND ANALYSIS OF COGNITIVE METHODS	50
8.3.1	<i>Experimental Investigation of Autonomous Medium Access</i>	50
8.3.2	<i>Experimental Investigation of Cooperative Medium Access</i>	55
8.3.3	<i>Experimental Investigation of Interference Signal Classification</i>	61
8.4	RECOMMENDATIONS FOR COGNITIVE METHODS.....	74
8.4.1	<i>Implementation Aspects.....</i>	74
8.4.2	<i>Cognitive Methods Recommendations.....</i>	75
8.5	CONCLUSION AND FUTURE WORK.....	77
9	VERWERTBARKEIT DER ERGEBNISSE	79
10	FORTSCHRITT DES WISSENSCHAFTLICHEN UND TECHNISCHEN STANDS WÄHREND DER LAUFZEIT DES FORSCHUNGSPROJEKTS	80
11	VERÖFFENTLICHUNG DER ERGEBNISSE	81
12	ANHANG	82
12.1	LITERATURVERZEICHNIS	83
12.2	ABKÜRZUNGSVERZEICHNIS	88

3 Aufgabenstellung des Forschungsprojekts

Nach zaghafte Anfängen Mitte der 90er Jahre haben sich industrielle Wireless-Technologien zu unverzichtbaren Komponenten der industriellen IT-Infrastruktur entwickelt. Diese Wireless-Systeme zeichnen sich durch den Einsatz unterschiedlicher Funktechnologien aus, weil keine Technologie allen Anforderungen gerecht wird. Dabei werden fast ausschließlich Technologie-Standards verwendet, die auch im Konsumbereich verwendet werden.

Die wichtigsten industriell genutzten Standards sind: IEEE 802.11x (WLAN), Bluetooth und WISA basierend auf IEEE 802.15.1, ZigBee bzw. IEEE 802.15.4. Alle arbeiten im Frequenzbereich 2,40 ... 2,48 GHz. Bei einem Parallelbetrieb müssen sich diese heterogenen Funktechnologien die Ressourcen Raum, Frequenz und Zeit teilen.

Das Koexistenzverhalten ist daher der entscheidende und damit begrenzende Systemparameter. Es hat sich gezeigt, dass das Koexistenzverhalten oft einen stärkeren Einfluss auf die Qualität der Datenübertragung hat als die passiven Effekte des Funkkanals, die durch Mehrwegeausbreitung und Bewegungseffekte hervorgerufen werden.

Um mögliche Beeinträchtigungen einer vitalen industriellen Funkanwendung zu vermeiden, übernehmen in Fabrikhallen Funknetzplaner eine manuelle Koordination und Überwachung. Dazu gehören die Auswahl geeigneter Funksysteme, deren Installation und die Überwachung des Betriebes. Gemeldete Betriebsstörungen werden auf mögliche Koexistenzkonflikte überprüft und geeignet abgestellt. Das kann dazu führen, dass einer Prioritätsliste folgend einige Funksysteme aufgrund unzureichender Koexistenzeigenschaften entfernt oder erst gar nicht zugelassen werden. Damit werden letztlich die mit der Funkkommunikation verbundenen wirtschaftlichen Möglichkeiten nicht ausgeschöpft.

Im Rahmen dieses Forschungsprojekts sollten Lösungsansätze durch die Erforschung neuartiger koexistenzoptimierter Funksysteme auf der Basis kognitiver Ansätze erforscht werden, um die bekannten Probleme des koexistenzlimitierten Betriebs heterogener Funksysteme in industriellen Einsatzszenarien zu vermeiden.

Die erarbeiteten Ergebnisse sollten umfangreich wissenschaftlich publiziert und den geeigneten industriellen Fachausschüssen (ZVEI-Arbeitskreis 'Wireless Automation', GMA-Fachausschuss 5.21 'Funkgestützte Kommunikation') zugänglich gemacht werden. Dadurch können die erarbeiteten Methoden zeitnah in die Entwicklung neuartiger und die Verbesserung bestehender kommerzieller industrieller Funkprodukte einfließen.

4 Voraussetzungen des Forschungsprojekts

Die Arbeiten wurden im Forschungsinstitut für industrielle Informationstechnik (inIT, www.init-owl.de) der Hochschule OWL durchgeführt. Es ist ein In-Institut des Fachbereichs Elektrotechnik und Technische Informatik. Es eine der führenden Forschungseinrichtungen auf dem Gebiet der industriellen Informationstechnik und beschäftigt derzeit mehr als 60 Mitarbeiter. Hier arbeiten sieben Professoren mit teilweise überlappenden Arbeitsgebieten in den Bereichen industrielle Echtzeitkommunikation, industrielle Bildverarbeitung und verteilte Echtzeit-Software. Im Forschungsschwerpunkt "Industrial Wireless" beschäftigen sich zurzeit vier Professoren und 20 wissenschaftliche Mitarbeiter mit aktuellen forschungsbasierten Fragestellungen.

Das Institut inIT ist zugleich eines der führenden Institute im BMBF-Spitzencluster „Intelligente technische Systeme OstwestfalenLippe – it's OWL". Es ist beheimatet unter dem Dach des Forschungs- und Entwicklungszentrum CENTRUM INDUSTRIAL IT (CIIT) auf dem Campus der Hochschule OWL in Lemgo. Das CIIT ist Deutschlands erstes Science-to-Business-Center im Bereich der industriellen Automation. Unter einem Dach arbeiten und forschen voneinander unabhängige Unternehmen und Institute an der Verknüpfung von Informations- und Automatisierungs-Welt. (www.ciit-owl.de)

5 Planung und Ablauf des Forschungsprojekts

Tab. 1 zeigt die Projektstruktur des Forschungsvorhabens. Neben dem Projektmanagement (Arbeitspaket 1 - AP 1) und der Erstellung von Dokumentationen und Publikationen (AP 7), sind fünf inhaltliche Arbeitsschwerpunkte vorgesehen, deren Beschreibung ebenfalls der Tabelle 1 entnommen werden kann.

Tabelle 1: Projektplan

AP 1	Projektmanagement (Projekt- und Kostenverfolgung)
AP 2	Leistungsbewertung adaptiver Verfahren Durch geeignete Simulationen und ergänzenden Messungen soll die Leistungsfähigkeit der zur Zeit diskutierten adaptiven Verfahren Detect and Avoid (DAA), Detect and Suppress (DAS) und Detect and Reduce (DAR) bewertet werden.
AP 3	Auswahl und Bewertung kognitiver Verfahren Erprobung und Auswahl einer geeigneten Funkkanalsensorik; Detektion und Klassifizierung von bestehenden Primärsystemen; Prädiktion des zukünftigen Verhaltens; Ressourcenauswahl des kognitiven Sekundärsystems für ein optimales Betriebsverhalten mit minimaler Störung bestehender Primärsysteme.
AP 4	Aufbau von Demonstratoren Es sollen zunächst mögliche Demonstratorkonzepte betrachtet werden: schmalbandiges HF-Front-End; breitbandiges HF-Front-End, Post-Processing-System. Für die Verifikation der erforschten Algorithmen ist ein geeignetes Demonstratorkonzept aufzubauen.
AP 5	Erprobungsmessungen / Leistungsbewertung Erprobungsmessungen mit den Demonstratoren mit implementierten kognitiven bzw. adaptiven Algorithmen; vergleichende Bewertung adaptiver und kognitiver Verfahren.
AP 6	Entwicklung von Algorithmen unter Implementierungsaspekten Es sollen effiziente kognitive Algorithmen unter Einbeziehung der Transceiver-Technologie entwickelt werden.
AP 7	Dokumentation und Publikation (Zwischenberichte, Abschlussbericht, Publikationen)

Der Zeit und Meilensteinplan ist aus Tabelle 2 ersichtlich.

Tabelle 2: Zeit- und Meilensteinplan

	1. Jahr				2. Jahr				3. Jahr			
	Q1	Q2	Q3	Q4	Q1	Q2	Q3	Q4	Q1	Q2	Q3	Q4
AP 1 Projektmanagement												
AP 2 Adaptive Verfahren												
AP 3 Kognitive Verfahren												
AP 4 Demonstratoren												
AP 5 Leistungsbewertung												
AP 6 Entwickl. Algorithmen												
AP 7 Dokumentation												
Meilensteine												
	M 1			M 2			M 3		M 4		M 5	M 6

Wichtige Eckdaten und Meilensteine sind:

- M 1: **Projektbeginn**
- M 2: Abschluss AP 2 (**Leistungsbewertung adaptiver Verfahren abgeschlossen**)
- M 3: Abschluss AP 3 (**Auswahl und Bewertung kognitiver Verfahren abgeschlossen**)
- M 4: Abschluss AP 5 (**Erprobungsmessungen / Leistungsbewertung abgeschlossen**)
- M 5: Abschluss AP 6 (**Entwicklung der Algorithmen fertig gestellt**)
- M 6: **Projektabschluss**

6 Wissenschaftlicher und technischer Stand

Koexistenzbeeinträchtigungen im industriellen Umfeld und deren Vermeidung sind ausgiebig von den relevanten Interessengruppen diskutiert und im ZVEI-Dokument [1] beschrieben.

Hierbei geht es im Wesentlichen um die Nutzung des lizenz- und gebührenfreien 2,4-GHz-Frequenzbereichs (2,40 ... 2,48 GHz), der sich einer weltweiten Nutzung erfreut. Als ISM-Band (industrial, scientific, medical) wird es vielfältig genutzt: Industrieanwendungen, medizinische Anwendungen, Heimanwendungen und Modellfernsteuerungen nutzen dieses attraktive Band gemeinsam. Koexistenzuntersuchungen und -probleme sind umfangreich in der Literatur beschrieben [2], [3], [4], [5], [6], [7], [8], [9], [10], [11], [12], [13] und [14].

Zur Vermeidung von Koexistenzbeeinträchtigungen wird in den einschlägigen Fachnormen eine manuelle Koexistenzplanung und/oder die Anwendung geeigneter adaptiver Mechanismen gefordert. Ziel dieser Ansätze ist eine "möglichst friedliche" Nutzung des gemeinsamen Mediums "Luft" durch mehrere auch unterschiedliche Funkssysteme im selben Raumbereich. Doch die Realität zeigt, dass Hersteller die Anwendung adaptiver Verfahren stets lediglich zur Optimierung der eigenen Funktionalität betreiben. Die mögliche Beeinträchtigung anderer Funkssysteme ist nicht Gegenstand der Optimierung.

Die Aktualität der Problematik unterstreicht eine Internetmeldung von elektroniknet.de [2]: "Europäische Kommission plant zwingende Zugriffskontrolle ab 10 mW Sendeleistung · Droht dem 2,4-GHz-Band Ungemach? Bluetooth, ZigBee und WiFi nutzen das frei zugängliche Frequenzband um 2,4 GHz. Weil auch ISM-Anwendungen und Radio-LANs (RLAN) hier unterwegs sind, steigt das Störpotenzial. Deshalb will die EU den Zugriff mit mehr als 10 mW über ein zwingend vorgeschriebenes Media Access Protocol regulieren." Dies bedeutet, dass der bisherige Betrieb laut harmonisierte Norm EN300328 mit Sendeleistungen bis zu 100 mW zukünftig nur noch mit adaptiven Mechanismen möglich sein soll. Dies wird allerdings zur Zeit diskutiert. Eine Entscheidung ist bisher noch nicht gefallen. Grundsätzlich verlangt die Norm EN 300 328 (Version 1.7.1) bereits heute die Anwendung von Medienzugangsmechanismen in den Produkten. Allerdings sind diese im Standard nicht explizit definiert.

Die für das Inverkehrbringen von Funksystemen maßgebende R&TTE-Richtlinie verlangt im Artikel 3, Absatz 2 die 'effektive Nutzung des Funkspektrums'. Die Einhaltung dieser Anforderung kann laut Amtsblatt der EU mit Einhaltung der harmonisierten Norm EN 300328 v1.7.1 lediglich vermutet werden.

Der mit diesem Vorhaben vorgeschlagene kognitive Ansatz geht letztlich einen entscheidenden Schritt über die adaptiven Mechanismen hinaus. Zu den *adaptiven Verfahren* zählen:

- Detect and Avoid (DAA): z.B. adaptive frequency hopping (AFH) bei Bluetooth. Es erfolgt ein Kanalwechsel bei Kanalbelegung.
- Detect and Suppress (DAS): z.B. listen before talk (LBT) bei CSMA/CA (carrier sense multiple access / collision avoidance). Es wird gewartet bis der Kanal frei ist.
- Detect and Reduce (DAR). Es wird im Fall der Kanalbelegung mit einer reduzierten

Leistung gesendet.

Kognitive Verfahren nutzen die funktionalen Elemente Detektion, Klassifizierung, Prädiktion und Ressourcenzuweisung. Aber auch selbstlernende Algorithmen aus dem Bereich der künstlichen Intelligenz (AI) gehören dazu und können die kognitiven Fähigkeiten beträchtlich erweitern. Vereinfacht ausgedrückt sind kognitive Verfahren somit 'intelligente' adaptive Verfahren.

Nichtkognitive Verfahren zur Koexistenzoptimierung werden in [3], [15], [16], [17], [18], [19], [20] und [21] beschrieben. Die bisherigen Forschungsarbeiten im Bereich der kognitiven Funkssysteme konzentrieren sich im Wesentlichen auf die Erhöhung der spektralen Effizienz im Bereich des Mobilfunks und der Bereitstellung von multilingualen Funkssystemen. Veröffentlichte Arbeiten zu kognitiven Ansätzen zur Koexistenzoptimierung sind in [22], [23], [24], [25], [26], [27] und [28] zu finden. Diese Arbeiten liefern vereinzelt hier nutzbare Ansätze. Doch keine der veröffentlichten Arbeiten betrachtet industrielle Applikationen mit den erforderlichen zeitlichen Randbedingungen 'strikte Echtzeit' und 'minimale Latenz'.

7 Zusammenarbeit mit anderen Stellen

Das Forschungsvorhaben wurde in enger Kooperation mit der Firma Phoenix Contact Electronics, der Firma Weidmüller und der Universität Rostock durchgeführt. Alle Projektpartner sind Mitglied in den Industriefachausschüssen

- GMA-Fachausschuss 5.21 'Funkgestützte Kommunikation' im Verein Deutscher Ingenieure e.V. (VDI);
- Arbeitskreis 'Wireless Automation', ZVEI - Zentralverband Elektrotechnik- und Elektronikindustrie e.V. .

Dadurch konnten bereits während der Projektlaufzeit zahlreiche Diskussionen mit interessierten Industriepartnern erfolgen. Somit wurde ein optimaler Wissens- und Technologietransfer zwischen Hochschule und Industrie sicher gestellt.

Außerdem werden die Ergebnisse den geeigneten industriellen Fachausschüssen (ZVEI-Arbeitskreis 'Wireless Automation', GMA-Fachausschuss 5.21 'Funkgestützte Kommunikation') zugänglich gemacht. Hierbei wird auch die ökonomische Verwertbarkeit der Ergebnisse konsequent verfolgt.

8 Ergebnisse des Forschungsprojekts – *Results of the Research Project*

The research project KOSYS faces coexistence issues of wireless medium access methods (MAMs). The focus is on the license-free 2.4 GHz ISM (industrial, scientific and medical) radio band which is shared by numerous wireless technologies.

Within the research project multiple sub-topics are highlighted. In the following sections, the results of the sub-topics are presented and discussed in more detail.

First of all, current advanced medium access methods (called adaptive methods) are analyzed and their performance is evaluated (Section 8.1). Based on the results, more intelligent medium access methods (cognitive methods) were designed (Section 8.2). Then the cognitive methods are implemented and also their performance is evaluated (Section 8.3). Based on the results of the performance evaluation of cognitive methods, conclusions are derived to advise future design of wireless medium access methods (Section 8.4). Finally, the results are summarized and future work is highlighted (Section 8.5).

8.1 Performance Evaluation of Adaptive Methods

Mainly three different types of adaptive methods shall be evaluated: Detect and Avoid (DAA), Detect and Suppress (DAS) and Detect and Reduce (DAR). The methods differ in the dimension they react if the channel is occupied. DAA methods react in the frequency dimension by switching the operating frequency, DAS method react in the time dimension by delaying its transmission, and DAR methods react in the power domain by reducing the transmission power.

The following section discusses performance evaluation approaches for wireless medium access methods. Then, a section is about current adaptive methods in standards for wireless industrial applications. The following section introduces the simulative investigation and the test scenario for the performance evaluation. Then, a section is about the measures and the goals of the performance evaluation. The final section shows the performance evaluation results.

8.1.1 Evaluation Approaches

Recently, many papers and scientific projects focus on adaptive methods for wireless media access. They aim to evaluate different adaptive methods with mainly three approaches: Verification by analytical discussion, by simulation with software tools and by measurements. It follows a discussion of important approaches.

8.1.1.1 Analysis Approach

The analytical verification of adaptive methods mostly are based on the well-known paper published by Bianchi in 2000 [29]. He used a probability model to determine the PER for carrier sense multiple access with collision avoidance (CSMA/CA) of IEEE 802.11. The paper is well-known for its straight-forward model approach. Nevertheless, the approach has some drawbacks. Bianchi assumes a negligible radio channel, which cannot be assumed especially for industrial application. Further, Bianchi assumes a homogeneous wireless network holding only IEEE 802.11 devices. Still the complexity of the model is huge, which makes the extension to a mutual interfering heterogeneous network much more difficult.

Based on Bianchi's approach, Shin et. al. published some papers for the analysis of heterogeneous networks. They presented a general framework in [30], and applied it for PER analysis of IEEE 802.15.4 devices interfered by IEEE 802.11b devices in [31], and for analysis of IEEE 802.15.4 interfered by multiple Bluetooth piconets in [32]. In contrast to Bianchi's approach they introduced a radio channel model, which is a log-distance path loss model using a fixed path loss exponent. It enables to model the PER as a function of spatial parameters. Therefore, spatial parameters are used to determine the signal to interference plus noise ratio (SINR). Based on the SINR the bit error ratio (BER) can be concluded. Using the BER in combination with the time of collision results in modeling the PER. So, the PER is a function of the time of collision and BER, which depends on the SINR derived from spatial parameters and power levels.

The approach benefits from an improved radio channel model, which results in a more accurate PER estimation. But the approach suffers from an assumption made to reduce the

complexity of the analytical model. The authors assume that each wireless system (IEEE 802.15.4, IEEE 802.11b and Bluetooth piconets) are hidden to each other and therefore they work independent. But to evaluate different adaptive methods for media access they should have mutual interference.

8.1.1.2 Simulation Approach

Additionally to complex analytical discussions, many papers validate adaptive methods using simulations. An important discussion was published by Schimschar et. al. in [33] and [34]. They simulate networks with devices based on the standard European Norm EN300328 to evaluate extreme cases, which are allowed. Their simulation is based on petri nets. They focused on simulation from the industrial point of view. Therefore, the result show next to the PER also the transmission time, which is an important parameter for industrial applications. Although the papers show the extreme cases, they do not really represent wireless devices based on industrial standards such as IEEE 802.15.4. Additionally, they do not discuss the efficiency of the communication.

8.1.1.3 Experimental Approach

In comparison to analysis and simulations, there were only a few measurements performed to evaluate adaptive methods. The reason are that the environment is non-negligible and that often some simple assumptions are applied to omit tests. One often applied assumption is that a transmitted packet is interfered when the received power of the desired signal is less than the power of an interfering signal, while otherwise there is no interference. This assumption gives an idea of the performance, but it neglects many parameters such as the receiving filter bandwidth and error correction.

Some papers try to evaluate the weakness of the assumptions. For example [35] evaluates the interference impact between IEEE 802.15.4 and IEEE 802.11. The authors disprove the assumption that IEEE 802.15.4 interferes only IEEE 802.11 when it doesn't use CSMA/CA. So, even if IEEE 802.15.4 uses the adaptive method CSMA/CA, it disturbs IEEE 802.11 communication to some extent. Further, the authors prove that measurements are necessary for validation of heterogeneous networks using adaptive methods.

8.1.2 Adaptive Methods in Standards

Many wireless technologies which are standardized use adaptive methods. In the following sections well-accepted industrial standards are listed.

8.1.2.1 IEEE 802.15.4 using CSMA/CA

A global accepted standard for industrial wireless application is IEEE 802.15.4 [36]. IEEE 802.15.4 defines the first and the second layer from the OSI model for low-rate wireless personal area networks (WPANs). Some wireless technologies are based on (a subset of) IEEE 802.15.4. The standard is designed to enable low-cost devices with low-power consumption. So, example industrial applications are wireless sensor and actor networks, which can be powered by batteries. The MAC of IEEE 802.15.4 defines the adaptive methods CSMA/CA or ALOHA. While CSMA/CA requires sensing mechanism, ALOHA only delays the

channel access for a random period. So, IEEE 802.15.4 defines only adaptive methods based on DAS.

8.1.2.2 WirelessHART without Adaptive Methods

A wireless technology, which is used in industrial applications especially in process automation is WirelessHART [37]. It is also based on IEEE 802.15.4, but it doesn't use any adaptive methods. Because it adapts only a subset of IEEE 802.15.4 which describes a PHY and leaves out all MAC regulations of IEEE 802.15.4 including CSMA/CA and ALOHA.

8.1.2.3 IEEE 802.11 using CSMA/CA

Another wireless technology which is used in industrial applications as well as in home and office application is IEEE 802.11 [38] called WLAN. WLAN is widespread standard for high-rate communication. In comparison to IEEE 802.15.4, WLAN isn't designed for low-power sensor and actor networks. WLAN's default channel access method is the adaptive method CSMA/CA, which is mandatory for all WLAN devices. So, before an arbitrary devices wants to send, it delays its transmission for a random period. While delaying, the channel is sensed the whole time. If the channel change to a busy state, the delaying is continued when the channel is free again. If a transmitted packet is interfered, then the range of the maximum possible delaying period is increased. But to avoid ending in infinity delay periods, the standard defines an upper limit. This channel access method is summarized using the term basic access.

Additionally to basic access, the standard defines an acknowledged version. So, after delaying a random period just before transmitting the data packet, which could be big amount of data, the device transmits a short request data packet called request to send (RTS). In the case of no interference, the destination device answers with a short ready packet called clear to send (CTS). Then the original data packet can be send with a high probability of no interference. The RTS/CTS variant reduces the time the channel is occupied by an interference, because only short RTS can be interfered. But it suffers from an additional overhead, which (theoretically) reduces the maximum possible data rate.

Another variant of basic access method is the method introduced in IEEE 802.11e [39] which is now part of [38]. It is a prioritized variant of CSMA/CA which is backward compatible to the basic access method. The variant defines four quality of service classes. Each class has a different probability to delay the data transmission for a short period than another device. This variant requires to classify data packets to its priority, which requires the configuration of each device.

8.1.2.4 Bluetooth/IEEE 802.15.1 using AFH

Additionally to IEEE 802.15.4, Bluetooth [40] is a widespread industrial WPAN standard. The first two layers are also part of an IEEE standard, namely IEEE 802.15.1 [41]. In contrast to IEEE 802.15.4, Bluetooth faces high-rate communication. For modulation it uses frequency hopping spectrum spreading (FHSS) with 79 channels, which enables to use a DAA as adaptive method. In the version 1.2 Bluetooth introduced such adaptive method called adaptive frequency hopping (AFH). With AFH the master device in a network (piconet) is able

to avoid some of the channels. Therefore, all channels have to be classified. The implementation for classifying channels is vendor-specific. After some channels are considered as bad for example based on the PER of the specific channels, the master device generates a channel map of usable channels and advise its clients to apply the new channel map at a pre-definite time. AFH is especially good for avoiding stationary spectrum users such as WLAN and IEEE 802.15.4. But because of the vendor-specific implementation, the coexistence improvement AFH is not deterministic.

8.1.2.5 Summary

The adaptive methods used by wireless technologies are summarized in Table 1. Only wireless technologies are discussed which are used in industrial applications. While DAS and DAA are in use, the authors don't know any nonproprietary industrial wireless technology which uses a DAR adaptive method.

Table 1: Standards using adaptive methods

Standard	Reference	Type	Adaptive Method
IEEE 802.15.4	[36]	DAS	CSMA/CA or ALOHA
WirelessHART	[37]	-	-
IEEE 802.11	[38]	DAS	(prioritized) CSMA/CA with optional RTS/CTS
Bluetooth v1.2	[40]	DAA	AFH
IEEE 802.15.1	[41]	DAA	AFH

8.1.3 Simulative Investigation

The evaluation of MAMs was performed using a simulation. There are mainly two types of simulation: Discrete-time simulation and discrete-event simulation. Discrete-time simulation computes values per time step for each signal. Signals interconnect two ports such as antenna ports of radio devices. Discrete-time simulation is the choice to model signals with ordinary differential equations (ODEs) and differential algebraic equations (DAEs), and therefore is good for modeling physical effects of wireless channels such as multi-path effects and modulation.

But using discrete-time simulation for a wireless network with several radio devices each using a finite state machine (FSM) to adapt to the wireless channel's state results in a huge and complex model. Most of the computation focus on negligible physical effects. For example the propagation time is negligible in a simulation focusing on media access. Even if two devices have a large distance of $d = 500m$, then the propagation delay t_p results only to:

$$t_p = \frac{d}{c_0} = \frac{500m}{3 * 10^8 m/s} = 1.67\mu s \quad (1)$$

This is very small in comparison to typical packet durations of more than 1ms. So, discrete-time simulation has a large overhead in terms of modeling complexity and computation.

Another type of simulation is the discrete-event simulation. Discrete-event simulation only operate for some time steps, which are called events. So, on each event some computation is performed. This type of simulation is optimal for modeling FSM and packet orientated network simulations. Many network simulation projects use discrete-event simulation tools. The tools also provide many well tested libraries for fast and accurate modeling of wireless technologies, wireless channels, mobility and movement. The main disadvantage of discrete-event simulation for modeling wireless communication is that the physical effects of the wireless channel aren't as accurate as with discrete-time simulation. Nevertheless, many libraries model physical effects and their impact on the communication well.

We decided to simulate the above introduced test scenarios with a discrete-event simulation tool called OMNeT++. OMNeT++ is a discrete event based simulation framework which is used already by numerous projects for wired and wireless packet based network simulations. A project focusing on wireless communication and its various aspects is MiXiM. It was chosen for the evaluation. MiXiM provides modules to simulate multiple wireless nodes in a radio environment.

Each wireless node consists of four layers: application layer, network layer, MAC layer and physical layer. The application layer generates the application payload which has to be transmitted or received from another wireless node. Then, the network layer handles the packet addressing for the network. The next layer, called MAC layer, adds the MAC address by interaction with an additional module called the address resolution protocol (ARP) module. Further, the MAC layer handles the medium access. Finally, the physical layer transmits the packet to the other wireless nodes. The physical layer itself consists of an analogue model and a decider model. The analogue model simulates the physical channel behavior such as the channel attenuation. The decider model is responsible for packet loss decision. It neglects or accepts received packets based on the outcome of the analogue model. Each layer module consists of four interfaces: one data and one control interface to the preceding and one data and one control interface to the succeeding layer. Hence, the layers are message oriented state machines.

Additionally to the wireless node, MiXiM handles two modules for the radio environment: the connection manager and the world module. The connection manager handles the packet forwarding from a transmitting wireless node to all wireless nodes in the coverage range. To compute the coverage range, it has a simple logarithmic path loss model. The second module is the world module. The world module holds the properties of the radio environment such as the spatial dimension of the environment.

8.1.3.1 Measurement Interface

IA applications require deterministic MAMs. Hence, the above discussed goals are declared for all layers starting from the medium access control layer (MAC).

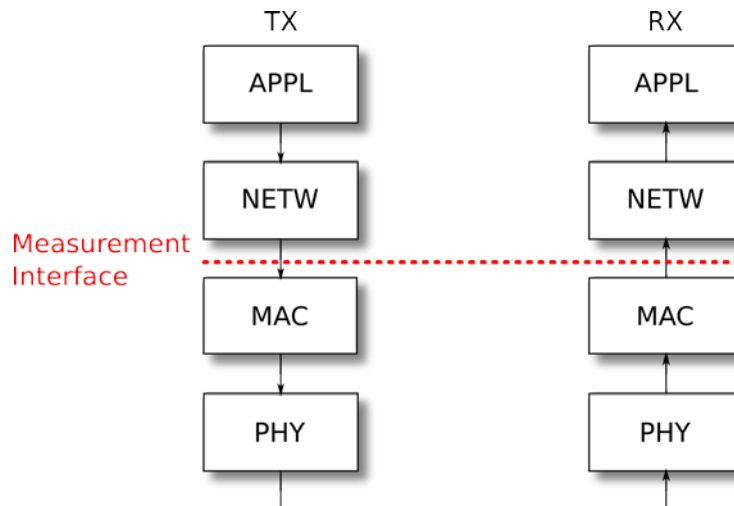


Figure 1: Measurement interface right above the MAC

According to Figure 1, it includes the MAC and the physical layer (PHY). The measurements are performed at the device under test (DUT) transmitter (TX) and receiver (RX) right below the network layer (NETW).

8.1.3.2 Radio Channel: Logarithmic Path Loss Model

As mentioned above the physical layer contains an analogue model. The purpose is to compute the reception power. The reception power P_{RX} is the multiplication of the transmission power P_{TX} with the path loss PL . Therefore, the model has to compute the path loss.

According Table 2, a time- and frequency-invariant path loss model is sufficient. Therefore, we chose a simple path loss model, which determines the path loss PL according to

$$PL = \frac{P_{TX}}{P_{RX}} = \frac{(4\pi)^2 d^n}{\lambda^2} \quad (2)$$

With the wavelength λ , the transmitter-to-receiver distance d and the path loss exponent n . The path loss model does not model any frequency nor time variant effects.

8.1.3.3 Packet Loss Decision: Modulation-based Decider

The physical layer contains a decider model following the analogue model. Its purpose is to decide which packets are lost based on the outcome of the analogue model. The chosen analogue model returns a time-independent reception power of the incoming packet. A decider is chosen which determines a packet loss based on the SINR value and the applied modulation type.

Firstly, the SINR value is determined:

$$SINR = \frac{P_{Signal}}{P_{Noise} + P_{Int1} + P_{Int2} + P_{Int3} + \dots} \quad (3)$$

With the reception power of the desired packet P_{Signal} , the noise power P_{Noise} and the reception power of the interfering packets $P_{Int1}, P_{Int2}, P_{Int3}, \dots$

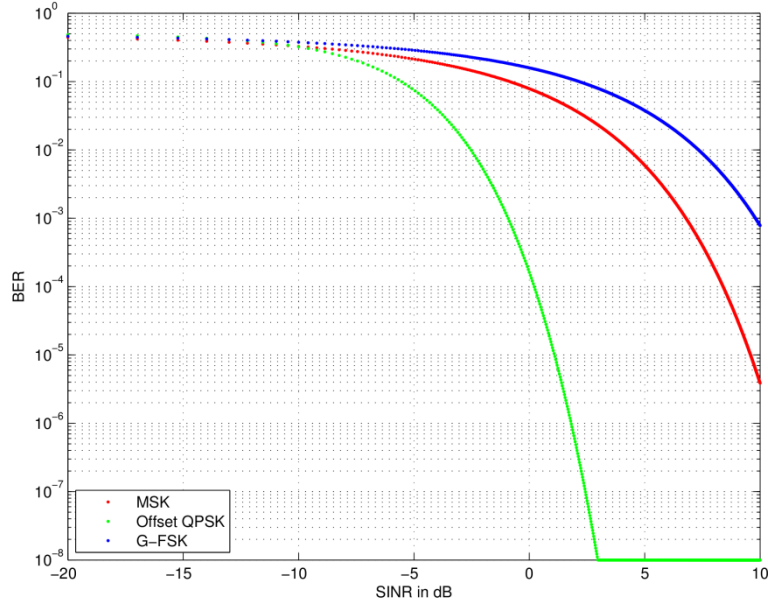


Figure 2: Bit error rate from the SINR for some modulation types

Then, the bit error probability P_B can be concluded as

$$P_B = f_{modx}(SINR) \quad (4)$$

Where $f_{modx}()$ returns the bit error probability for modulation type $modx$. The bit error probability, which is assumed equal to the bit error rate, for some modulation types is shown in Figure 2.

After determining the bit error probability, the packet loss probability P_p can be determined. It can be concluded from the packet length in bits l such that

$$P_p = 1 - (1 - P_B)^l. \quad (5)$$

Hence, a packet is neglected in the simulation if a uniform random number $0 \leq x \leq 1$ is below the packet loss probability P_p such that

$$x < P_p \quad (6)$$

8.1.3.4 Simulation Scenario: Indoor Process Plant

The evaluation of MAMs shall be performed from an IA perspective. Hence, the indoor process plant environment is chosen as radio environment according to [42]. The applied

parameters are listed in Table 2. Further, the simulation scenario is adjusted for evaluation purpose.

Table 2: Parameter for the Indoor Process Plant Environment

Parameter	Value
Spatial dimension	100m x 25m
Intervisibility	NLOS/OLOS
Path loss exponent	3.5
DUT	IEEE 802.15.4
DUT communication topology	Peer-To-Peer
Number of DUT wireless nodes	100 TX/RX pairs
DUT payload length	1000 Byte
DUT initiation of data transfer	Cyclic
DUT transmission interval	4s
IX	IEEE 802.11
IX communication topology	Broadcasting
Number of IX wireless nodes	50

The simulation contains mainly two types of wireless nodes: DUTs and interfering (IX) devices. The DUTs are the wireless nodes which are evaluated. The IX devices are the wireless nodes which disturb the communication of the DUTs.

According to Table 2, the environment expects DUT pairs of TX and RX wireless nodes. Hence, the communication topology is peer-to-peer. Therefore, each pair communication is interfered by the other 99 DUT TX/RX pairs using the same wireless technology and 50 IX

devices using a different wireless technology. Further, it can be concluded that there is a one-way communication without any receiver response, i.e. no acknowledgement.

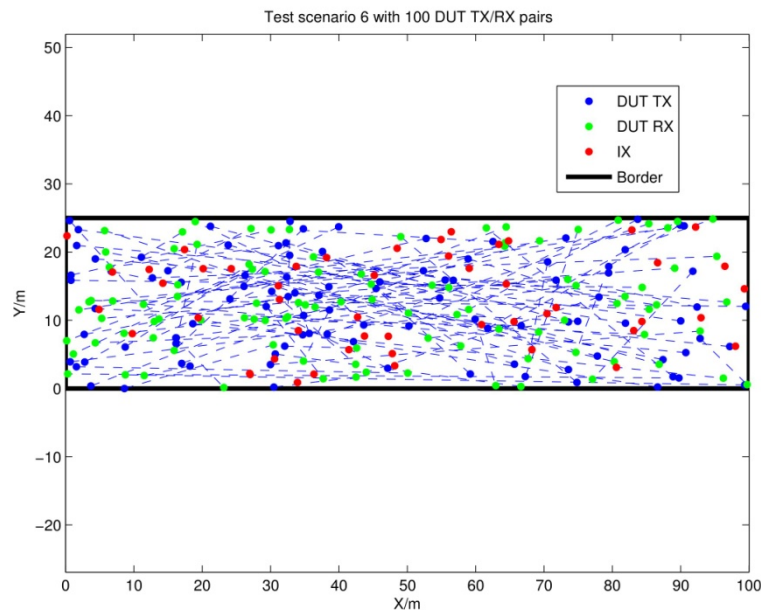


Figure 3: Spatial positions for the simulation with 100 DUT TX/RX pairs and 50 interfering devices

Figure 3 shows an example spatial distribution for 100 DUT TX/RX pairs and 50 IX devices. Each DUT TX (blue dot) is connected (blue dashed line) with the corresponding DUT RX (green dot). Further, the IX devices (red dots) are also shown. Also the spatial dimensions are shown by the border (black solid line). The spatial distribution itself varies randomly for each simulation.

The packets are generated in the application layer. According to Table 2, the generation is performed in a cyclic manner. The initial packet generation is randomly delayed. The random delay is chosen to simulate balanced steady-state spectrum utilization.

8.1.3.5 Non-Adaptive Medium Access Method: IEEE 802.15.4 GTS

The indoor process plant environment is used to evaluate the MAMs. According Table 2, the payload is relative small and the transmission interval therefore high. Hence, a low-rate wireless technology such as IEEE 802.15.4 is chosen (see [36]). IEEE 802.15.4 has mainly two different MAMs: contention based MAM and slot based MAM. The contention-based MAM is an adaptive MAM while the slot based MAM is a non-adaptive MAM. The latter uses some guaranteed time slots (GTS) which is equivalent to a simple time division multiple access (TDMA). Hence, the non-adaptive MAM accesses the medium in a fixed cyclic manner without any adaption. The parameters are mentioned in Table 3.

Table 3: Parameter of the Non-Adaptive Medium Access Method of IEEE 802.15.4

Parameter	Value
-----------	-------

Medium access method	TDMA
Transmission power	10 mW
Center frequency	2405 MHz
Bandwidth	5 MHz
Bitrate	250 kBit/s
Payload length	1000 Byte
Total header length	14 Byte

8.1.3.6 Adaptive Medium Access Method: IEEE 802.15.4 CSMA/CA

As mentioned above the DUT uses IEEE 805.15.4. The adaptive MAM is the contention-based CSMA/CA. Therefore, the adaptive MAM accesses the medium using a random backoff time and checks if the medium is in idle-state before data transmission is started [2]. The parameters are mentioned in Table 4.

Table 4: Parameter of the Adaptive Medium Access Method of IEEE 802.15.4

Parameter	Value
Medium access method	IEEE 802.15.4 CSMA/CA
Transmission power	10 mW
Center frequency	2405 MHz
Bandwidth	5 MHz
Bitrate	250 kBit/s
Payload length	1000 Byte

Total header length	14 Byte
---------------------	---------

8.1.3.7 Medium Access Method of the Interfering Device: IEEE 802.11 CSMA/CA

Additional to the DUT TX/RX pairs, the medium is also utilized by the IX devices. Typically in a process plant environment wireless nodes are based on IEEE 802.11 (see [38]). Therefore, the IX devices use the CSMA/CA MAM of IEEE 802.11 (see Table 2). Mainly, the IXs are broadcasting the packets without requiring any response such as an acknowledgement. The parameters are mentioned in Table 5.

Table 5: Parameter of the Medium Access Method of the Interfering Device IEEE 802.11

Parameter	Value
Medium access method	IEEE 802.11 CSMA/CA
Transmission power	100 mW
Center frequency	2412 MHz
Bandwidth	22 MHz
Bitrate	11 MBit/s
Total length	64 Byte

8.1.4 Performance Evaluation Measures

The research project faces the evaluation of adaptive MAMs to discover the limitations from the IA perspective. As mentioned in the introduction, IA applications require a reliable and deterministic MAM. Hence, it results into two goals:

1. Successful packet transmission has to be guaranteed.
2. The packet reception has to be finished within a maximum time limit. This time limit shall be known in advance.

The two goals will be discussed in detail in the following sections.

8.1.4.1 Goal 1: Successful Packet Transmission

The first goal could be expressed in terms of packet loss rate (PLR) such that for an optimal MAM

$$PLR \rightarrow 0. \quad (7)$$

PLR = 0 is identical to maximum system availability $A = 100\%$. The goal impacts the system's throughput r_{TP} which is

$$r_{TP} = N_{TX} * \frac{L_{Payload}}{T_{Packet}} * (1 - PLR), \quad (8)$$

with N_{TX} transmitting devices, a constant packet duration T_{Packet} and the payload length $L_{Payload}$. Hence, the throughput limit in terms of packet transmission $r_{TP,MaxTx}$ could be expressed as

$$r_{TP,MaxTx} = N_{TX} * \frac{L_{Payload}}{T_{Packet}}. \quad (9)$$

Further, the system's throughput is limited by the spatial, time and spectrum capacity. In the same time duration, spatial position and spectrum it is possible to receive one packet only. In the simplified case that each radio device is using the same spatial and spectrum capacity, it can be assumed that the maximum throughput appears when all packets are transmitted right after each other without any time gap in between. Neglecting propagation delays, the throughput limit in terms of packet reception $r_{TP,MaxRx}$ results to

$$r_{TP,MaxRx} = \frac{L_{Payload}}{L_{Header} + L_{Payload}} * r_B, \quad (10)$$

with the bit length of the packet's header L_{Header} and the bitrate r_B .

Summarizing, the throughput is below $r_{TP,MaxTx}$ and $r_{TP,MaxRx}$. Therefore, the throughput limit is the minimum of $r_{TP,MaxTx}$ and $r_{TP,MaxRx}$:

$$r_{TP} \rightarrow \min(r_{TP,MaxTx}, r_{TP,MaxRx}) \quad (11)$$

It results to

$$r_{TP} \rightarrow \min\left(N_{TX} * \frac{L_{Payload}}{T_{Packet}}, \frac{L_{Payload}}{L_{Header} + L_{Payload}} * r_B\right). \quad (12)$$

Therefore, the first goal is met if the system's throughput is independent of PLR until it reaches the maximum reception capacity.

8.1.4.2 Goal 2: Deterministic Transmission Time

The second goal is to ensure packet reception within a certain time range and determine the maximal transmission time. According to Figure 4, the transmission time t_T is the corresponding time parameter. Hence, the goal can be expressed as

$$t_T < T_{T,Threshold}, \quad (13)$$

Where $T_{T,Threshold}$ is a specified upper threshold for transmission time.

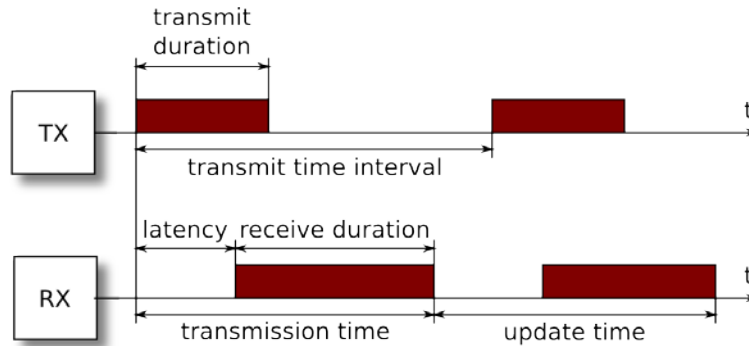


Figure 4: Time parameter

To reduce the effort of evaluating simulations and measurements, the goal can be simplified to

$$P_{95\%}(t_T) < T_{T,P95-Threshold}, \quad (14)$$

where $P_{95\%}(x)$ denotes the 95% percentile value of x , which returns the value that is right above 95% of the values. Hence, the second goal is met if 95% of the transmission time measurements return a value below the threshold $T_{T,P95-Threshold}$.

8.1.5 Performance Evaluation Results

This section shows the results of the performance evaluation of adaptive methods using simulative investigations.

The evaluation is performed using the above discussed simulation. The result consists mainly of two parts: the system's data throughput and the transmission time. The results will be discussed while the number of DUT wireless nodes is varying. The variation shall show when the capacity limit is reached. Hence, with an increasing number of wireless nodes, the interference impact raises.

The first goal is about the system's data throughput. The goal for the throughput mentioned in equation (9) is to receive all transmitted packets up to the maximum reception capacity. Figure 5 shows the system's throughput for the adaptive and the non-adaptive MAM. In the figure, the green and red line show the throughput limits $r_{TP,MaxRx}$ and $r_{TP,MaxTx}$, respectively. The dark and light blue marks show the throughput results for the adaptive and non-adaptive MAM case, respectively.

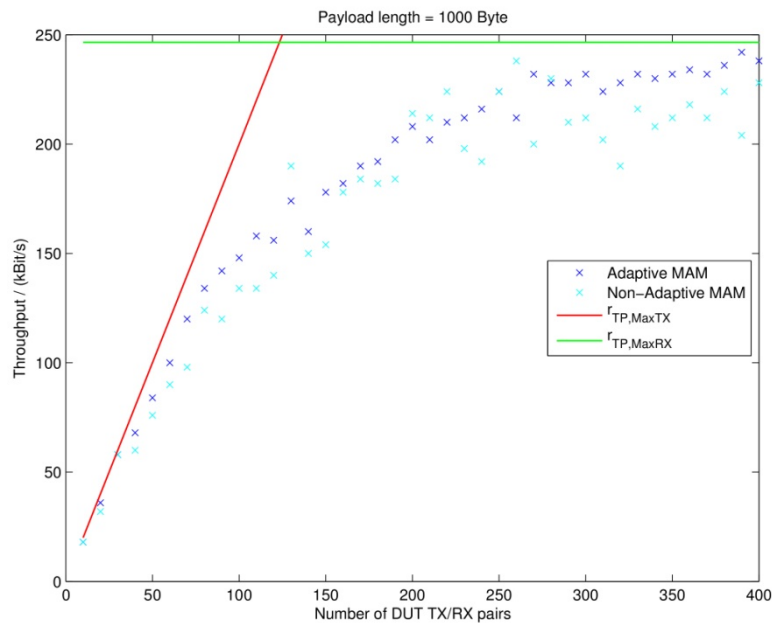


Figure 5: Throughput for Adaptive and Non-Adaptive MAM

The difference between the throughput and the limit defined by equation (12) is shown in Figure 6, which is called throughput gap. The results show a maximum at the intersection of the limits $r_{TP,MaxRx}$ and $r_{TP,MaxTx}$, which is approximately at 120 DUT TX/RX pairs. The maximum throughput gap of the non-adaptive MAM has the value of 100 kBit/s while the maximum throughput gap of the adaptive MAM reaches only 86.5 kBit/s. Therefore, the adaptive MAM shows an improvement of 13.5 kBit/s. Further, it can be concluded that the adaptive MAM performs better because in 34 out of 40 simulations the throughput gap is lower.

The adaptive MAM shows an additional improvement, because it uses only 64.9% of the maximum system's throughput in the worst case. It can be concluded, that there is still a large gap for improvements, e.g. by cognitive MAMs.

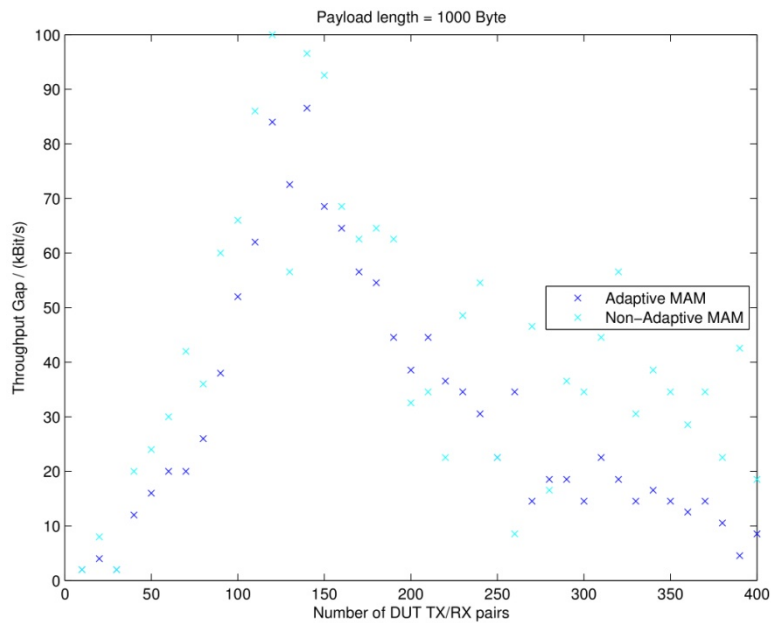


Figure 6: Throughput Gap for Adaptive and Non-Adaptive MAM

The second goal addresses the transmission time. The goal as mentioned in equation (14) is a transmission time with a 95% percentile value below a threshold. In Figure 7, the values are shown for the adaptive and the non-adaptive MAM. It is important to notice that only successful received packets are considered. Further, no acknowledgement techniques are applied and therefore it considers one-way communication.

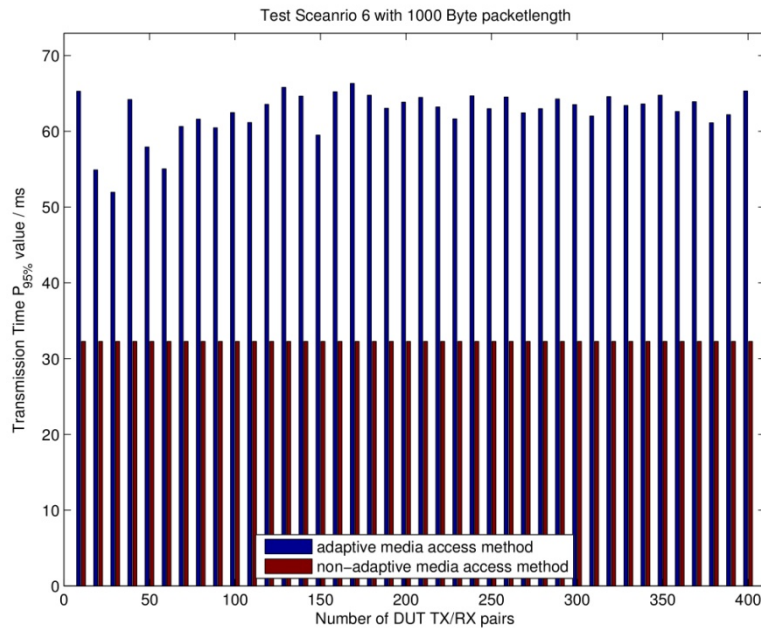


Figure 7: Percentile 95% of the Transmission Time

In the case of the non-adaptive MAM, the transmission time is deterministic and its 95% percentile value varies only minimal. The transmission time consists mainly of the fixed packet duration and the distance-dependent propagation delay. The propagation delay is

varying up to 200 *ns*, which corresponds to 60 *m* free space distance. The ratio between the variation and the mean value is 6.2 *ppm*, which shows that the propagation delay impact is negligible. Hence, the non-adaptive MAM results in a deterministic transmission time.

The second case, the adaptive MAM, results in a much higher variation. Additionally to the packet duration and the propagation delay, the transmission time contains a contention window and the duration for clear channel assessment (CCA). The 95% percentile value of the transmission time varies up to 14.4 *ms*. The ratio between the variation and the mean value results to 23%, which shows that the variation impact is not negligible. Therefore, the adaptive MAM fulfills the equation (14) only if the threshold $T_{T,P95-Threshold}$ is larger than the 95% percentile value of the transmission time.

The final conclusion is twofold. While the adaptive MAM performance is closer to the first goal, the non-adaptive MAM reaches the second goal easily. But both MAMs do not achieve both goals. Therefore, a novel MAM is required, which combines the benefits of both MAMs.

8.2 Coexistence Optimization with Cognitive Methods

Adaptive MAMs react upon certain events such as packet loss or channel state transition in order to mitigate the interference. In contrast to the reactive nature of adaptive MAMs, cognitive MAMs are based on proactive approaches. They try to model the radio environment and adapt the wireless communication accordingly in order to lower the packet loss rate, increase spectrum efficiency, lower communication latency or to fulfill some application requirements. They sense frequency channels, predict future channel occupancy, negotiate channel occupancy information, and tune its operation parameter adequately.

From the architecture point of view cognitive MAMs can be divided into two categories: Cooperative and autonomous methods.

In the following sections cognitive methods for coexistence optimization are introduced and discussed.

8.2.1 Cognitive Methods for Autonomous Medium Access

We evaluate three cognitive approaches for autonomous MAMs. The methods are based on two different probabilistic models – Markov model and auto-regressive model – in order to predict future channel occupancy. We evaluate them with measurements in IA worst case scenarios.

8.2.1.1 Markov Model based Predictive Medium Access

To model the time behavior of a wireless channel, it has to be observed for a certain amount of time. In IA applications, mostly narrowband transceiver modules are used to transmit IA control data. Therefore, the received signal strength indicator (RSSI) is an appropriate measure for observing the channel occupancy. In the scenario the RSSI is sufficient for analysis. In more complex scenarios the SINR may be taken into account. To model the time behavior a sequence of RSSI samples has to be taken. An example of such an observed RSSI sequence is shown in Figure 8.

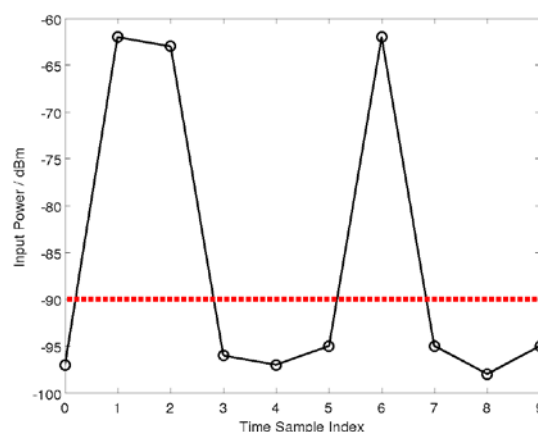


Figure 8: Observation sequence derived from RSSI samples

In order to determine the states represented by the RSSI measures, they have to be classified by e.g. applying a threshold. It results an observation sequence $O = (o_0, o_1, \dots, o_N)$ of states with $o_i \in S = \{0, 1\}$ for $i \in \{1, 2, \dots, N\}$ (see Figure 9). The observation sequence has to be finite because the common case of industrial wireless nodes have to predict the wireless channel occupancy and transmit real-time data with a single transceiver module.

O can be modeled as a first order Markov model (MM) [43] if two requirements are met. Firstly, O has to be a stationary process within the state space S . Secondly, the probabilistic property

$$\frac{P(o_{i+1} = s_{i+1} | o_i = s_i, o_{i-1} = s_{i-1}, \dots)}{P(o_{i+1} = s_{i+1} | o_i = s_i)} = \quad (15)$$

for all $s_j, o_j \in S$ is met. So, a succeeding observation only depends on the current observation.

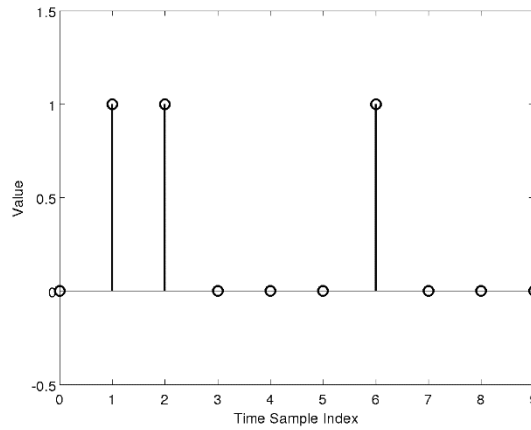


Figure 9: Binary sequence of observed states. '1' represents state 'busy' and '0' represents state 'idle'.

A MM consists of a finite set of states S , the initial probability distribution Π , and the transition probability distribution A .

The initial probability distribution defines a set of initial probabilities $\Pi = \{\pi_{s_0}, \pi_{s_1}, \dots\} \forall s_i \in S$. Each initial probability $\pi_{s_i} \in \Pi$ expresses the probability for a random observation o_i to be in state $s_i \in S$ as:

$$\pi_s = P(o_i = s_i) \quad (16)$$

The sum of all initial probabilities result in $\sum_{\forall s \in S} \pi_s = 1$. In case the observation sequence O is finite, it results in $\pi_s = N_s/N$ where N_s is the number of observations which are in state s . The initial probability distribution of the previous example is shown in Figure 10.

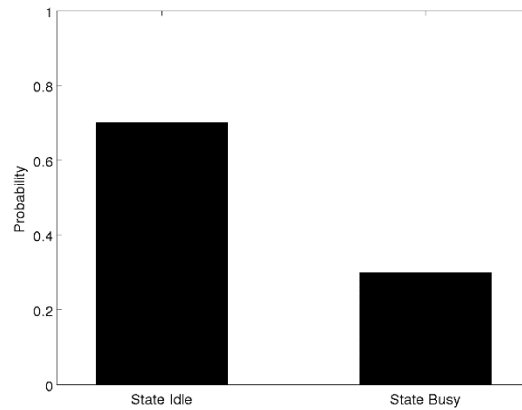


Figure 10: MM initial probability distribution

The transition probability $a_{src,dst} \in A$ expresses the probability for a certain observation o_i to transit from the source state $src \in S$ to the destination state $dst \in S$ for the subsequent observation o_{i+1} . It follows the conditional probability:

$$a_{src,dst} = P(o_{i+1} = dst | o_i = src) \quad (17)$$

The sum of all transition probabilities with the same source state $src \in S$ result in $\sum_{\forall dst \in S} a_{src,dst} = 1$. In case the observation sequence O is finite, it results in $a_{src,dst} = N_{src,dst} / (\sum_{\forall s \in S} N_{src,s})$ where $N_{x,y}$ is the count of transitions from state x to state y . The transition probability distribution of the previous example is shown in Figure 11.

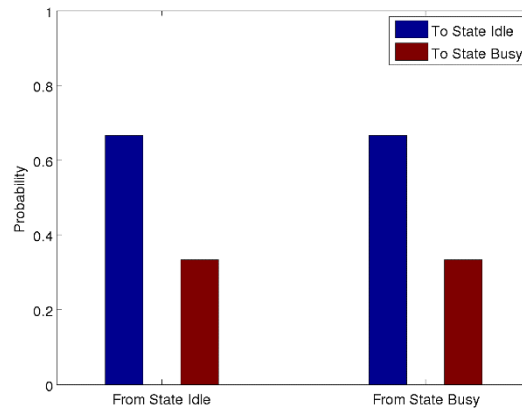


Figure 11: MM transition probability distribution

Given a certain MM with (S, Π, A) , the probability of a chosen sequence of states $(s_0, s_1, \dots, s_l) \in S^{l+1}$ can be expressed as:

$$P((s_0, s_1, \dots, s_l) | (S, \Pi, A)) = \pi_{s_0} \cdot a_{s_0, s_1} \cdot \dots \cdot a_{s_{l-1}, s_l} \quad (18)$$

So, the probability of an idle gap of two samples results in:

$$P((0, 0, 1) | (S, \Pi, A)) = \pi_0 \cdot a_{0,0} \cdot a_{0,0} \cdot a_{0,1} \quad (19)$$

In general, the probability of observing the state $s \in S = \{0,1\}$ for d subsequent observations before leaving the state can be expressed as:

$$P(D_{s,d}|(S, \Pi, A)) = \pi_s \cdot (1 - a_{s,s}) \cdot (a_{s,s})^d \quad (20)$$

Where $D_{s,d}$ represents the sequence $(s_0, s_1, \dots, s_{d-1}, s_d) \in S^{d+1}$ with $s = s_0 = s_1 = \dots = s_{d-1} \neq s_d$. Using the general expression, we define the term "MM average distance" \bar{d}_s of state s as:

$$\begin{aligned} \bar{d}_s &= \frac{1}{\pi_s} \sum_{d=0}^{\infty} d \cdot P(D_{s,d}|(S, \pi, A)) \\ &= (1 - a_{s,s}) \cdot \sum_{d=0}^{\infty} d \cdot (a_{s,s})^d \\ &= \frac{1}{1 - a_{s,s}}, \text{ if } a_{s,s} < 1 \end{aligned} \quad (21)$$

In case the observation sequence O is finite, it results in:

$$\bar{d}_s = \begin{cases} \frac{1}{1 - a_{s,s}}, & \text{if } a_{s,s} < 1 \\ N_s, & \text{else} \end{cases} \quad (22)$$

Where N_s is the number of samples which are in state s . The idle and busy MM average distances \bar{d}_0 and \bar{d}_1 of the previous example are shown in Figure 12.

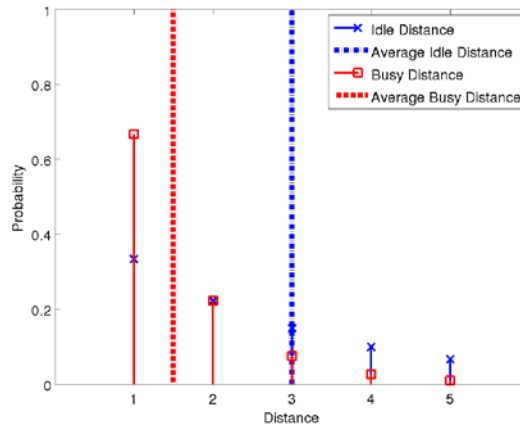


Figure 12: Idle and busy MM average distances

The distances may be used to imagine an average time behavior. Figure 13 shows a generated average time behavior starting with the busy state. It has a similarity of about 70% in comparison with the observation sequence shown in Figure 9. MM-based predictive MAMs may be applied in many different approaches. We focus on the two methods explained in [43]: MM2 and MM4. MM2 is only based on the initial idle probability π_0 , while MM4 is based on the MM average idle and busy distances \bar{d}_0 and \bar{d}_1 , respectively.

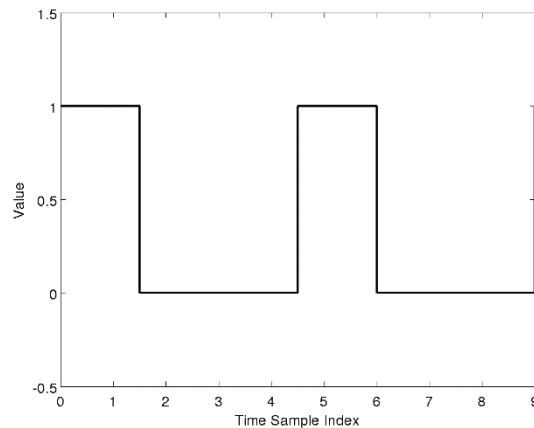


Figure 13: Example time behaviour based on MM average distances

8.2.1.2 Auto-Regressive Model based Predictive Medium Access

The auto-regressive (AR) model is a time series model which can be used to predict the next term of a given time series by a linear weighted sum of previous terms in the series. This paper provides only a brief introduction of the AR model to ease the understanding of this paper. The details of the AR model based predictive medium access is available in our papers [44] and [45] which suggests that, AR modelling is suitable for modelling the time behavior of an IEEE 802.11 based WLAN system.

AR modelling requires also a sequence of measured RSSI samples and classifying the channel states by applying a threshold value as seen in Figure 8. While MM considers only the current observation sequence, AR modelling is an iterative process, where (i) the model order is chosen, (ii) the model coefficients are determined and finally (iii) the current observation sequence is used for prediction. The model order (i) and the coefficients (ii) need to be related to a current primary user (PU) activity. Any changes of the PU result in a new set of AR coefficients.

The AR model is also known as an infinite impulse response (IIR) filter as it has memory and feedback. The AR model of order p , denoted by $AR(p)$, is defined as follows [46]:

$$X_t = \sum_{i=1}^p a_i X_{t-i} + \epsilon_t \quad (23)$$

Where a_i are the AR coefficients, X_t is the series under investigation, p is the order of the model and ϵ_t is the white noise error term.

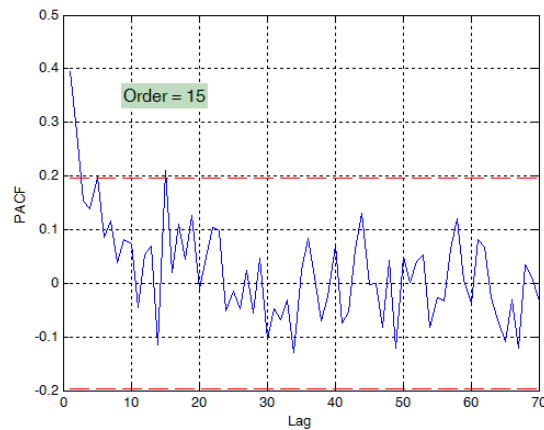


Figure 14: PACF for determining the AR model order

In the first step, the model order is chosen. The model order can be estimated by computing the partial autocorrelation function (PACF) of the time series data (Figure 14). The PACF of an AR (p) model is zero at lag $p + 1$, $p + 2$ and higher where p is the order of the AR model [46]. Practically, the value of PACF is not exactly zero for lags greater than p but fluctuates around zero. So, 80% confidence interval is used to estimate the order of the AR model. As seen in Figure 14, the PACF of the IEEE 802.11 time series data is within the 80% confidence interval after lag 15. So, the corresponding AR model order is 15.

In the second step, the model coefficients are determined. The coefficients $a = (a_1, a_2, \dots, a_p)$ can be estimated using the Yule-Walker equation which can be expressed in matrix form [46]:

$$a = \begin{bmatrix} 1 & r_1 & r_2 & \dots & r_{p-1} \\ r_1 & 1 & r_1 & \dots & r_{p-2} \\ \vdots & \vdots & \vdots & \dots & \vdots \\ r_{p-1} & r_{p-2} & r_{p-3} & \dots & 1 \end{bmatrix}^{-1} \begin{bmatrix} r_1 \\ r_2 \\ \vdots \\ r_p \end{bmatrix} \quad (24)$$

Where r_i is the autocorrelation coefficient at lag i .

In the final step, the current observation sequence is used for prediction based on the previous derived coefficients. After observing the sequence $O = (X_{t-p-1}, X_{t-p-2}, \dots, X_{t-1})$ with p samples, the very next sample X_t can be predicted:

$$X_t = \sum_{i=1}^p a_i X_{t-i} \quad (25)$$

Then, the next sample X_{t+1} can be concluded:

$$X_{t+1} = \sum_{i=1}^p a_i X_{t-i+1} \quad (26)$$

Proceeding in the same way, p future samples may be predicted to constitute the future sequence $F = (X_t, X_{t+1}, \dots, X_{t+p-1})$. From F some possible temporal white spaces (time gaps) may be derived.

8.2.2 Cognitive Methods for Cooperative Medium Access

Cognitive autonomous MAMs improve the performance of a single radio system opportunistically. While, cooperative systems negotiate the resource allocation and optimize the performance of several systems in a certain environment. This negotiation requires a communication opportunity, which can be achieved via a control channel (CC).

8.2.2.1 Inter-System Automatic Configuration Medium Access Method

We propose a novel MAM called inter-system automatic configuration MAM (ISAC MAM). The approach is operating between wireless systems, which is called the ISAC network. A wireless system is for example a wireless network based on IEEE 802.11 with one access point and several stations. For optimal operation, ISAC has to be supported by each system operating in the same frequency band.

ISAC's design has mainly three goals:

- a) Interference awareness
- b) Ensuring real-time and reliable communication
- c) Investment protection for existing wireless systems

The first goal is necessary for IA applications to provide the second goal, real-time performance and reliable communications. ISAC systems aim to avoid interference with other wireless systems and protect themselves from being interfered.

The third goal focuses on implementation requirements. The ISAC approach unifies the spectrum utilization management. It is suitable for being integrated into existing industrial wireless solutions such as industrial WLAN, Bluetooth, WirelessHART, ISA100.11A, and ZigBee. The integration of the approach shall be therefore simple with minor protocol adaption.

The ISAC network consist of two different entities: ISAC supervisor and ISAC client. The ISAC network requires a single central ISAC supervisor and permits multiple ISAC clients. The ISAC supervisor uses the CC for communication.

8.2.2.2 Supervisor

The most important entity in an ISAC network is the ISAC supervisors for resource management.

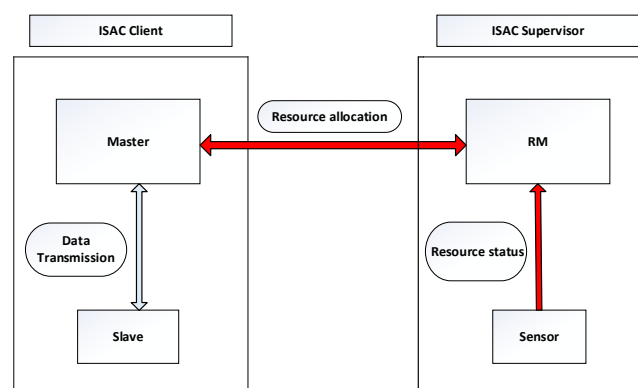


Figure 15. Basic ISAC network consist of ISAC supervisor and ISAC client connected via control channel (red arrows)

Thereby, the term resources refers to the hyperspace introduced in [47] consisting of multiple dimensions such as spectrum, time, code and the spatial dimension. The tasks of the ISAC supervisor are (i) resource allocation and (ii) interference mitigation. Therefore, it is equipped with the cognitive features of resource sensing and resource occupancy prediction.

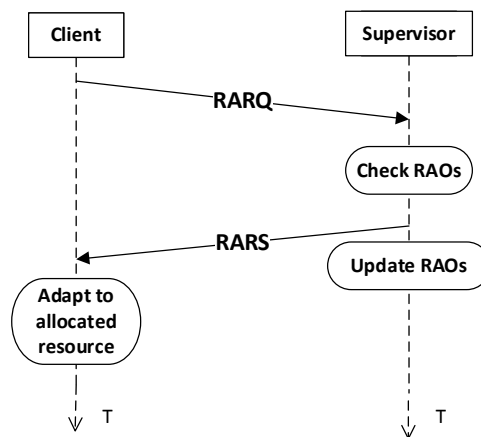


Figure 16. Sequence diagram of resource allocation negotiation between ISAC client and ISAC supervisor

As shown in Figure 15, the ISAC supervisor consists of two different wireless devices: Resource sensing device (sensor) and resource management device (RM). The sensor is responsible for resource sensing and predicting future behavior. Figure 16 shows the resource allocation negotiation procedure for two client. In case an ISAC client requests a resource allocation (RARQ), the RM selects the optimal resource allocation opportunity (RAO) according to the resource utilization capabilities of the ISAC client. Next, the RM response with the allocated resources (RARS) and the ISAC client tunes accordingly.

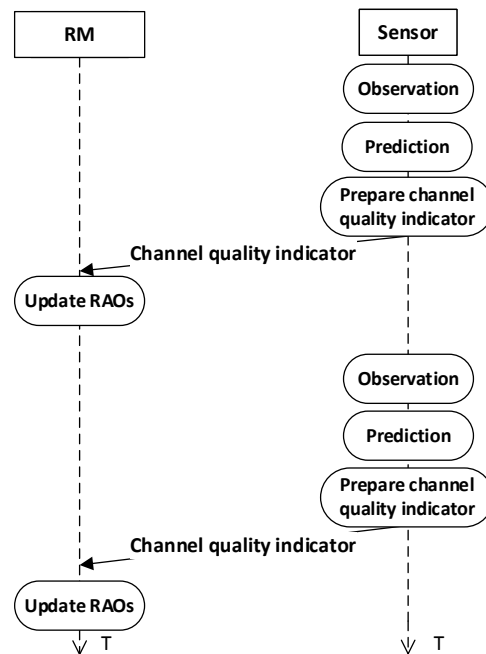


Figure 17. Sequence diagram of cyclic resource status reporting from sensor to resource manager

Additionally to resource allocation, the ISAC supervisor has to mitigate interferences, which could be either observed by the ISAC client or the ISAC supervisor's sensor. The sensor informs the RM about the resources status based on the resource sensing and prediction outcome. Then, the RM determines RAOs as illustrated in Figure 17. In case an ISAC client detects an interference within its utilized resources, it initiates a resource allocation negotiation within the limited resource utilization capabilities.

8.2.2.3 Client

The ISAC clients are resource users. The ISAC clients are independent wireless systems. In IA such wireless systems are Bluetooth piconets, WirelessHART mesh networks, or WLAN infrastructure networks. These wireless systems are used already for multiple applications like controlling or monitoring tasks. Each ISAC client has to provide a communication interface to the central ISAC supervisor. Typically, a good choice for the integration is the central management device of the certain wireless system like Bluetooth master, WirelessHART gateway, or WLAN access point, respectively.

The ISAC client's tasks are to (i) request for resource allocations from the ISAC supervisor and tune accordingly, and optionally to (ii) inform the ISAC supervisor about interferences. In order to reach the first task, the only mandatory requirement for the ISAC clients is to have tuning capabilities.

In order to reach the optional second task, the ISAC clients have to be equipped with sensing capabilities either listen-before-talk features such as WLAN and WirelessHART CSMA/CA or packet loss notification features. The sensing outcome can be used to initiate a resource allocation negotiation as mentioned above.

8.2.2.4 Control Channel

In general, a cognitive MAM needs to sense the spectrum and select an appropriate channel for the SU communication. To achieve this cooperatively, radio systems with cognitive MAMs communicate with each other via a CC [48]. Basically, the CC is a logical channel. Its implementation offers two possibilities:

1. Common control channel: The control messages are being exchanged on the same channel as used for the wireless solutions but during idle data phases. This solution is easy from a hardware point of view but requires a sophisticated time scheduling, which might conflict with desired real-time application.
2. Dedicated control channel: A separate physical channel is reserved for the exchange of control messages. Depending on the available hardware structure, the dedicated CC might use the same transceiver unit as the data messages. As mentioned before, the same sophisticated time scheduling is necessary. If two transceiver units for the data and control messages are available, the time scheduling is drastically simplified.

A separate transceiver unit might also support a wired CC if the application tolerates it. Further examples are given in [49].

Within ISAC, a CC is used for the communication with the ISAC supervisor. The ISAC concept requires a CC, which has to be always available for communication and therefore a dedicated CC. So, it has to be guaranteed that the CC never gets interfered by some PUs, SUs or any other kind of interferences.

8.2.3 Cognitive Methods for Interference Signal Classification

Cognitive methods require awareness about the environment, especially about interfering systems. Awareness about interfering systems is targeted by signal classification processes.

A signal classification process usually consists of several series-connected layers, as depicted in Figure 18. The input signal $x(t)$ is in general a superposition of the desired signal, various other unknown signals, and noise. Prominent signal features are extracted from this superposition, such as symbol rate, modulation, bandwidth etc., and used next as distinct features for the signal classifier. The classifier assigns input signals to different classes, here PU signal labeling, depending on the extracted information from the features.

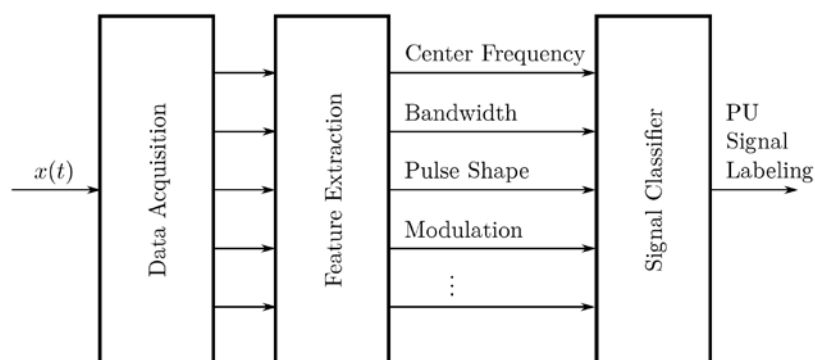


Figure 18: Signal classification process (adapted from [1])

A neuro-fuzzy signal classifier (NFSC) was proposed, which utilize a-priori known signal features to classify PU systems by utilizing fuzzy logic based rules [50]. The utilized distinct features are: (i) Center frequency, (ii) bandwidth, (iii) pulse shape, (iv) time behavior and (v) hop behavior of PU systems.

The NFSC consists of six layers, as depicted in Figure 19, where each layer is specialized for a single task. The functionality of each layer will be discussed in the following sub-sections.

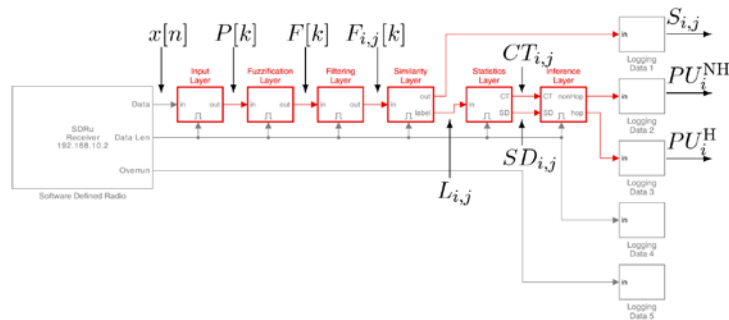


Figure 19: Overview of the NFSC implementation with six series-connected layers

8.2.3.1 Input Layer

In the first layer, a discrete logarithmic power density spectrum (PSD) is computed from the acquired discrete complex input signal, as depicted in Figure 20.

The discrete complex input signal represents in-phase and quadrature values. In general, from a discrete input signal $x[n]$ its continuous Fourier transform $X(\omega)$ is:

$$x[n] \xrightarrow{\mathcal{F}} X(\omega) \quad (277)$$

However, the practical implementation of the discrete Fourier transform on a computer nearly always uses the fast Fourier transform (FFT) algorithm. In this thesis, the FFT algorithm with some additional computations is applied to compute the desired discrete logarithmic PSD $P[k]$:

$$X[\omega] \mapsto P[k] \quad (288)$$

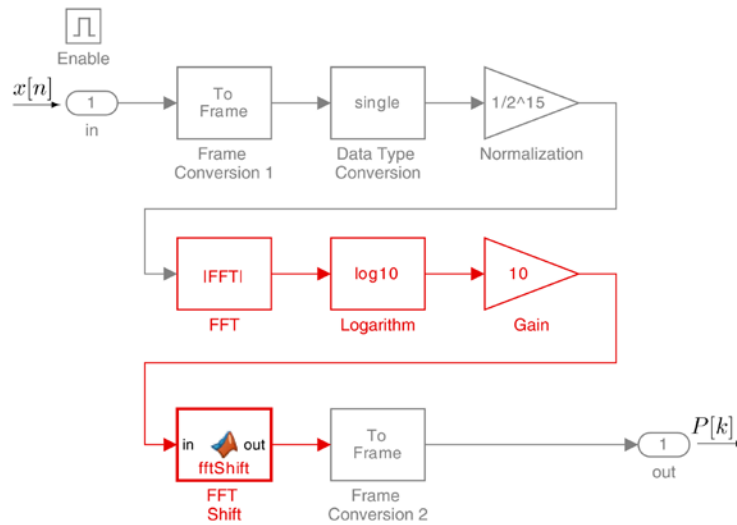


Figure 20: Input layer of the NFSC implementation

The computation of the discrete logarithmic PSD $P[k]$ is performed in a frame-based manner, depending on the selected FFT length 2^m , $m \in \mathbb{N}$.

An example of the frame-based processing is outlined in Figure 21. A rectangular window function is applied to the discrete input signal $x[n]$, that divides the input signal into 2^m samples-length non-overlapping frames. Subsequently, the discrete PSD of each frame is computed. Note, the iterator variable n describes discrete points in time, whereas k describes discrete frequency points in the spectral range.

The finite set K of all discrete frequency points k is:

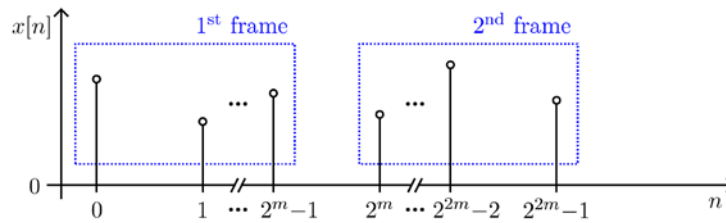
$$K = \left\{ 0, 1, \dots, \left(\frac{2^m}{2}\right), \left(\frac{2^m}{2} + 1\right), \left(\frac{2^m}{2} + 2\right), \dots, (2^m - 1) \right\} \quad (299)$$

and their corresponding discrete frequencies are described by the finite set of frequencies F^K :

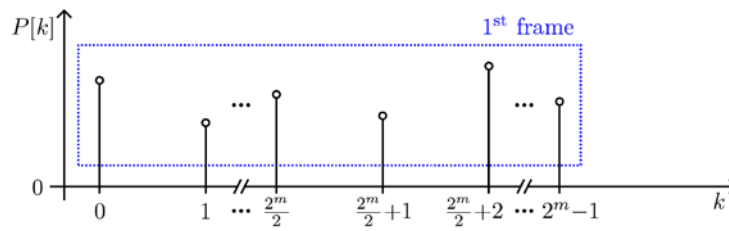
$$F^K = f^0 + \Delta f \cdot \left\{ \left(-\frac{2^m}{2} - 1\right), \left(-\frac{2^m}{2}\right), \dots, -1, 0, 1, \dots, \left(\frac{2^m}{2}\right) \right\} \quad (30)$$

Where f^0 is the selected center frequency and Δf is the resulting resolution bandwidth (RBW) of the PSD. The RBW Δf is the ratio of the bandwidth of the input signal, called display bandwidth B^{DI} , and the selected FFT length:

$$\Delta f = \frac{B^{DI}}{2^m - 1} \quad (31)$$



(a) Discrete input signal for input



(b) Discrete PSD as output

Figure 21: Example of frame-based processing

Since this thesis focuses on classifying PU systems in the 80 MHz wide 2.4-GHz-ISM radio band, all elements of the frequency set F^K lie within the continuous ISM radio band frequency interval $f^{ISM} = [2400,2480]$ MHz.

8.2.3.2 Fuzzification Layer

In the second layer, the incoming PSD frame is fuzzified by utilizing a specific membership function (MF), as depicted in Figure 22.

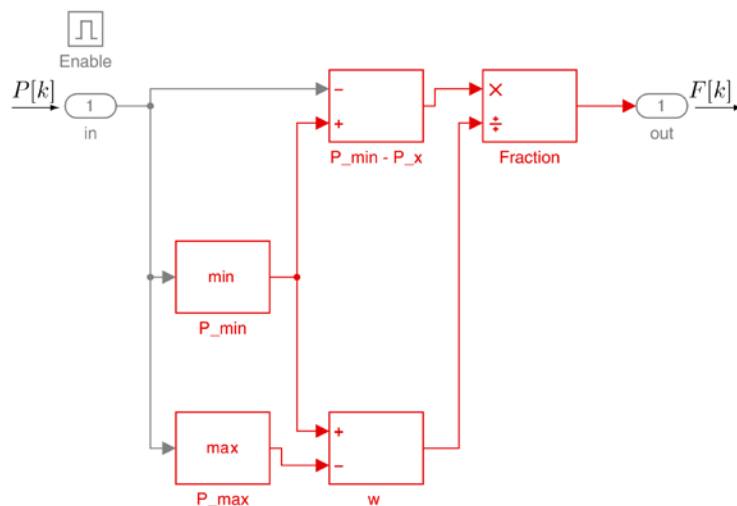


Figure 22: Fuzzification layer of the NFSC implementation

More precisely, with the MF $\mu^P[P[k]]$ the incoming PSD frame $P[k]$ is mapped to a membership value between zero and one:

$$\mu^P[P[k]]: U_P \rightarrow [0,1], P[k] \mapsto F[k] \quad (32)$$

Where U_P is the universe of discourse in terms of fuzzy logic for the PSD frame $P[k]$:

$$U_P = \{P_{\min} \leq P[k] \leq P_{\max} | k \in K\} \quad (33)$$

The applied specific MF is:

$$\mu^P[P[k]] = \left| \frac{P_{\min} - P[k]}{w} \right| \quad (34)$$

where w is the value range of the incoming PSD frame:

$$w = P_{\min} - P_{\max} \quad (35)$$

and P_{\min} is the minimum and P_{\max} the maximum value of the incoming PSD frame:

$$P_{\min} = \min(P[k]) \quad (36)$$

$$P_{\max} = \max(P[k]) \quad (37)$$

The resulting fuzzified PSD frame $F[P[k]]$ is a fuzzy set and can be written as:

$$F[k] = \{(k, \mu^P[k]) | k \in U_k\} \quad (38)$$

Where U_k is the universe of discourse for k , which is equal to the finite set K , compare eq. (3.3):

$$U_k = K \quad (39)$$

The membership function definition in eq. (3.7) can be rewritten through the simplification as:

$$\mu^P[k]: U_k \rightarrow [0,1], k \mapsto F[k] \quad (40)$$

The simplified fuzzified PSD frame $F[k]$ is named as fuzzy power spectrum (FPS) in this thesis.

8.2.3.3 Filtering Layer

The third layer filters the incoming FPS based on the PU system's frequency channels by a pulse shape selection, as depicted in Figure 23.

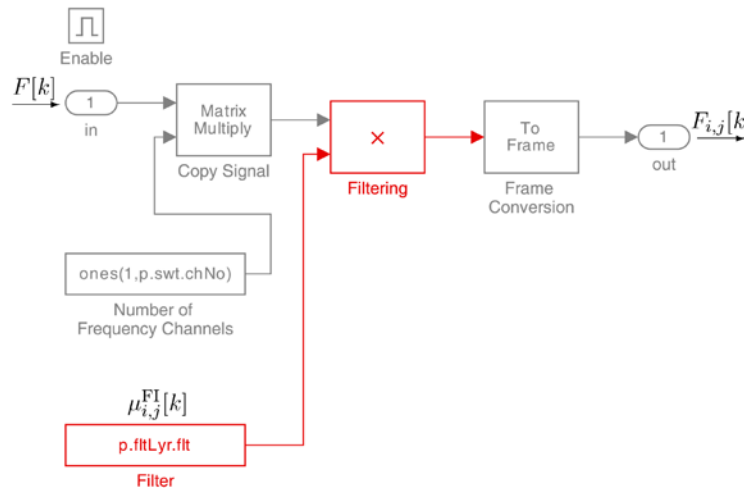


Figure 23: Filtering layer of the NFSC implementation

In particular, the incoming FPS $F[k]$ filtered over the j^{th} channel of the i^{th} respective PU system is represented as:

$$\mu_{i,j}^{\text{FI}}[k]: [0,1] \rightarrow [0,1], F[k] \mapsto F_{i,j}[k] \quad (41)$$

where $\mu_{i,j}^{\text{FI}}[k]$ is a fuzzy MF used as filter. For $\mu_{i,i}^{\text{FI}}[k]$ the pulse shape of the corresponding PU system is used, whereby in this thesis the following rectangular pulse shape was applied:

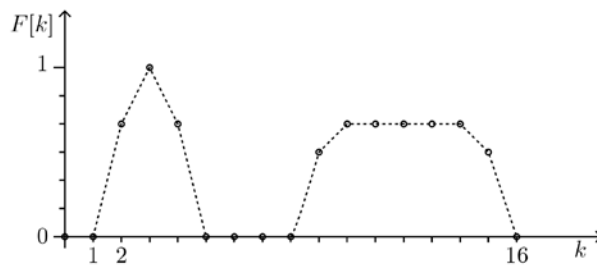
$$\mu_{i,j}^{\text{FI}}[k] = \text{rect}\left(\frac{f[k] - f_{i,j}^0}{D_i \cdot B_i^{\text{PU}}}\right) \quad (42)$$

The rectangular pulse shapes are depending on three parameters: (i) The channel bandwidth B_i^{PU} of the i^{th} PU system; (ii) the constant D_i , which can be selected to adjust the width of pass-band of the filter for the i^{th} PU system; and (iii) the center frequency $f_{i,j}^0$ of the j^{th} channel of the i^{th} respective PU system. Furthermore, the discrete frequency $f[k]$ is an element of the finite set of frequencies F^K , compare eq. (3.4).

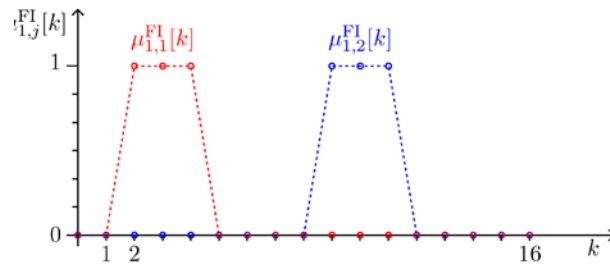
For a better understanding of the filtering, an example with one PU system, $i = 1$, is discussed next and depicted in Figure 24. It is assumed that the PU system has two frequency channels: $j = [1, 2]$.

An example FPS $F[k]$ is used as the input signal for the filtering layer, as depicted in Figure 24 (a). Since only one PU system with two frequency channels is considered, two example fuzzy MFs are sketched in Figure 24 (b). A rectangular pulse shape is chosen for both MFs, whereas the first one is described by $\mu_{1,1}^{\text{FI}}[k]$ and the second one by $\mu_{1,2}^{\text{FI}}[k]$.

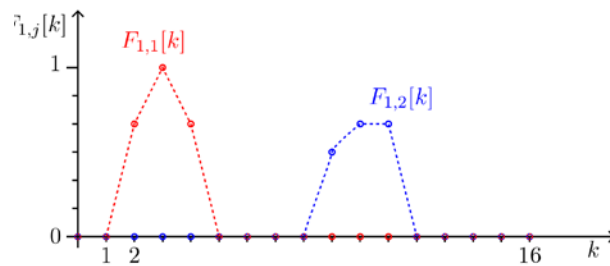
The two resulting filtered FPSs are presented in Figure 24 (c). In the first filtered FPS $F_{1,1}[k]$ is only the left side of the incoming FPS $F[k]$ present, whereas the right side of $F[k]$ is filtered out. On the other hand, the second filtered FPS $F_{1,2}[k]$ contains only a part of the right side of $F[k]$, whereas the left side of $F[k]$ is filtered out.



(a) Example of a fuzzy power spectrum



(b) Two example fuzzy membership functions



(c) Two filtered fuzzy power spectra

Figure 24: Example of filtering with one PU system and two frequency channels

8.2.3.4 Similarity Layer

The fourth layer measures the similarity between the incoming filtered FPS and the PU system's ideal pulse shape to evaluate the presence or absence of the corresponding PU system in a specific frequency channel, as depicted in Figure 25.

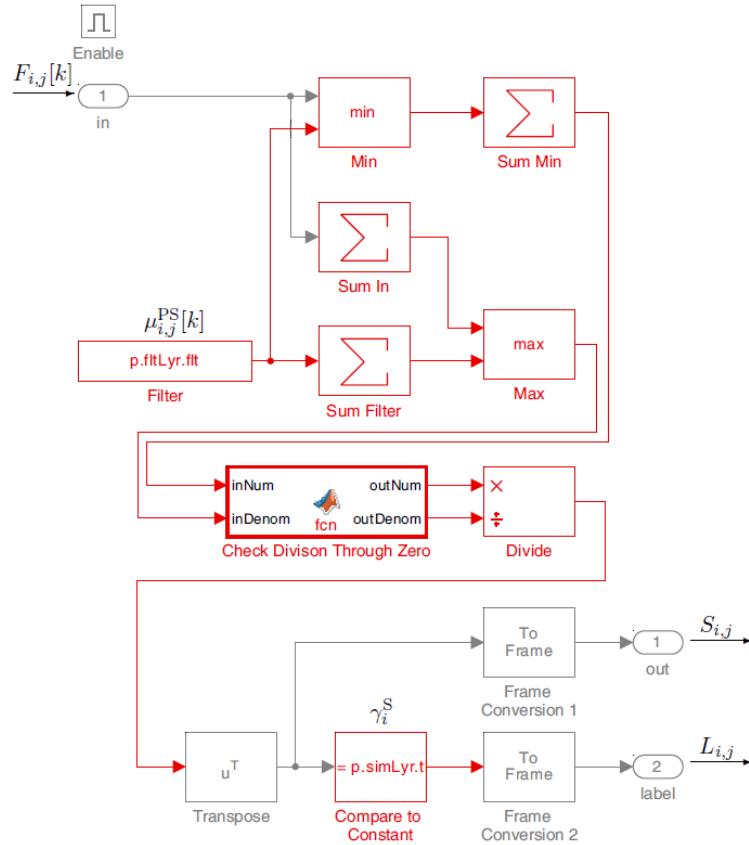


Figure 25: Similarity layer of the NFSC implementation

More exact, the similarity is measured by comparing the incoming filtered FPS $F_{i,j}$ with the ideal pulse shape $\mu_{i,j}^{\text{PS}}[k]$ of the respective PU system to generate a similarity measure (SM) score $S_{i,j}$ for each j^{th} channel of the i^{th} respective PU system.

The resulting SM score can be simply compared with a predefined threshold value to evaluate the presence or absence of the corresponding PU system. The comparison of the filtered FPS $F_{i,j}[k]$ with the ideal pulse shape $\mu_{i,j}^{\text{PS}}[k]$ is accomplished by computing the SM with the MF $\mu_{i,j}^{\text{S}}$:

$$S_{i,j} = \mu_{i,j}^{\text{S}} = \frac{\sum_{f \in U} \min(F_{i,j}[k], \mu_{i,j}^{\text{PS}}[k])}{\max(\sum_{f \in U} F_{i,j}[k], \sum_{f \in U} \mu_{i,j}^{\text{PS}}[k])} \quad (43)$$

where $S_{i,j}$ is the measure of the presence of the i^{th} PU system in its respective j^{th} channel. In other words, with the MF $\mu_{i,j}^{\text{S}}[k]$ the incoming filtered FPS $F_{i,j}[k]$ is mapped to a membership value between zero and one:

$$\mu_{i,j}^{\text{S}}: [0,1] \rightarrow [0,1], F_{i,j}[k] \mapsto S_{i,j} \quad (44)$$

In this thesis is the same rectangular pulse shape applied for the ideal pulse shape $\mu_{i,j}^{\text{PS}}[k]$ as the one for filtering, compare eq. (3.18), only the constant D_i is set to one, because here is the ideal pulse shape required.

The resulting SM score is a fuzzy set and can be written as:

$$S_{i,j} = \{(F_{i,j}[k], \mu_{i,j}^S) | F_{i,j}[k] \in [0,1]\} \quad (45)$$

where $S_{i,j}$ only contains one degree of membership. Elucidated, $S_{i,j}$ comprises only one single value, the degree of membership, for a specific i and j . As opposed to, for example, the fuzzy set $F_{i,j}[k]$, that contains an ordered set of fuzzy pairs $(k, \mu^P[k])$ for a specific i and j .

Next, this single value $S_{i,j}$ is compared with a predefined threshold value γ_i^S for each PU system, to categorically label the presence or absence of a PU system using the MF $\mu_{i,j}^L[S_{i,j}]$:

$$\begin{cases} 1, & \text{if } S_{i,j} \geq \gamma_i^S, \\ 0, & \text{otherwise.} \end{cases} \quad (46)$$

where $L_{i,j}$ is a binary time series representing SM layer labeling. Using fuzzy set notation it can be represented as:

$$L_{i,j} = \{(S_{i,j}, \mu_{i,j}^L[S_{i,j}]) | S_{i,j} \in [0,1]\} \quad (47)$$

Note, the label $L_{i,j}$ completely preserves frequency and time related information of an individual PU system. Hence, two very identical PU systems in terms of channel definitions can not be differentiated by the labels $L_{i,j}$. Center frequencies of the frequency channels, channel bandwidth, or the quantity of the frequency channels are such channel definitions. Therefore, another feature is introduced in the following last two layers in order to discriminate between those PU systems.

8.2.3.5 Statistics Layer

In the second last layer, two statistical measures are utilized, as depicted in Figure 26, in order to distinguish a hopping system from a non-hopping system, when two PU systems possess identical channel definitions.

Descriptive statistics summarize an entire data set to describe the main features of it. Central tendency (CT) and statistical dispersion (SD) are commonly applied, where the former measures the spread of data and the latter measures how the data is clustered around a single value.

On the one hand, transmissions of a hopping system are reasonably spread over its hopping channels and have a high SD as long as the total number of captured hops is fairly large. On the other hand, a non-hopping system exhibits high CT, since all transmissions are expected to be in a single frequency channel.

Non-hopping systems maintain cumulative moving average of incoming binary values $L_{i,j}$ as a measure of CT $CT_{i,j}$ as given by the MF $\mu_{i,j}^{CT}[L_{i,j}]$:

$$CT_{i,j} = \mu_{i,j}^{CT}[L_{i,j}] = \frac{L_{i,j} + ((q-1) \cdot CT_{i,j}^{prev})}{q} \quad (48)$$

Where q is the total number of process frames and $CT_{i,j}^{prev}$ is the previous computed measure of CT.

On the other side, only the first occurrence over each hopping channel is remembered for a hopping system as a measure of SD $SD_{i,j}$. It is given by the MF $\mu_{i,j}^{SD}[L_{i,j}]$:

$$SD_{i,j} = \mu_{i,j}^{SD}[L_{i,j}] = \begin{cases} 1, & \text{if } L_{i,j} = 1, \\ \text{unchanged,} & \text{otherwise.} \end{cases} \quad (49)$$

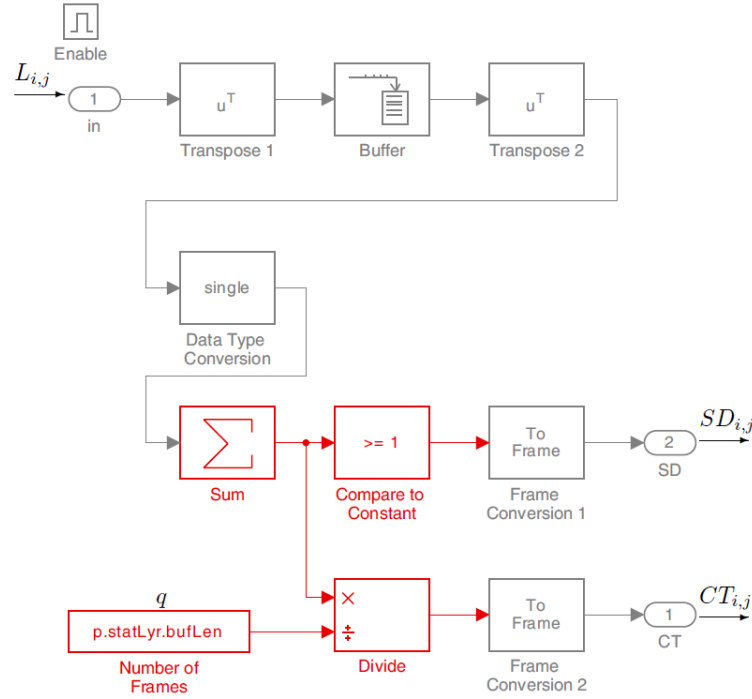


Figure 26: Statistics layer of the NFSC implementation

8.2.3.6 Inference Layer

Finally, in the last layer a decision is made whether a present PU system is a hopping or non-hopping system, as depicted in Figure 27.

On the one hand, the MF $\mu_i^{NH}[CT_{i,j}]$ is applied to evaluate the presence of a non-hopping PU System:

$$PU_i^{NH} = \mu_i^{NH}[CT_{i,j}] = \begin{cases} 1, & \text{if } \max(CT_{i,j}) \geq \gamma_i^{CT}, i = \text{const.} \\ 0, & \text{otherwise.} \end{cases} \quad (50)$$

where γ_i^{CT} is a specific threshold value for the i^{th} PU system.

On the other hand, the presence of a hopping PU system is evaluated the MF $\mu_i^H[SD_{i,j}]$:

$$PU_i^H = \mu_i^H[SD_{i,j}] = \begin{cases} 1, & \text{if } \text{mean}(SD_{i,j}) \geq \gamma_i^{SD}, i = \text{const.} \\ 0, & \text{otherwise.} \end{cases} \quad (51)$$

where γ_i^{SD} is a specific threshold value for the i^{th} PU system.

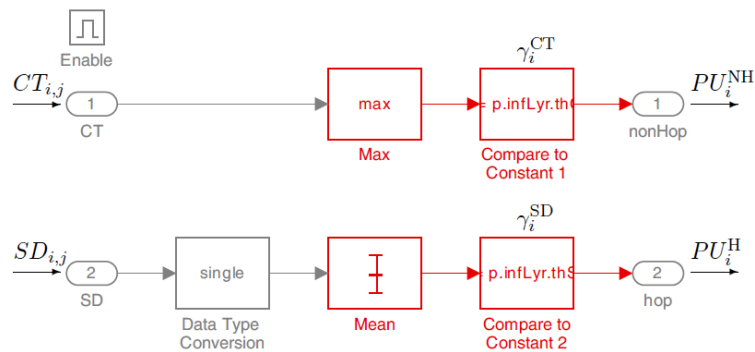


Figure 27: Inference layer of the NFSC implementation

8.2.3.7 Summary

In this section the NFSC approach was illustrated for a better understanding from the implementation perspective, see Figure 20 to Figure 27.

However, the original perspective of it is a neural network. A neural network comprises process elements, or neurons, which are interconnected to form a computation network. Each process element usually produces a single output value by accumulating inputs from other process elements.

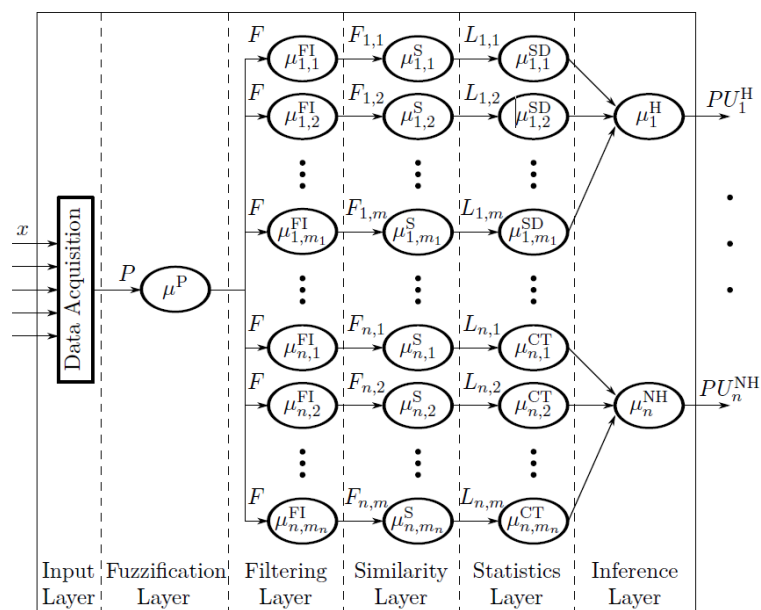


Figure 28: Block diagram of the NFSC (adapted from [50])

The original perspective is diagrammed in Figure 28. Input and fuzzification layer consists of only one process element each. The inference layer consists of two process elements for each PU system, thus for n PU systems there are $2n$ process elements in this layer. There is exactly one process element corresponding to each channel of each PU system in all other layers. Consequently, if m_i denotes the total number of frequency channels of the i^{th} PU system, then each of these layers contains $\sum_{i=1}^n m_i$ process elements.

8.3 Performance Evaluation and Analysis of Cognitive Methods

The cognitive methods from the previous section are experimentally evaluated. The experiments are discussed in this section including the setups, test scenarios, implementation, validation, measurement results and analysis.

8.3.1 Experimental Investigation of Autonomous Medium Access

In Section 8.2.1 cognitive methods for autonomous medium access are introduced. This section discusses their experimental evaluation.

According to IA applications, the master-slave architecture which is quite common in IA is selected as a test-bed implementation scenario. For simple testing purposes, the test-bed contains only two secondary users (SUs) in a master-slave constellation and one PU. Their antennas are placed in a test box. The test box is a shielded box lined with absorbers, which isolates the antennas from the external radio environment. Therefore, the test box approaches an ideal radio environment. The test-bed implementation is set in the test box as shown in Figure 29.

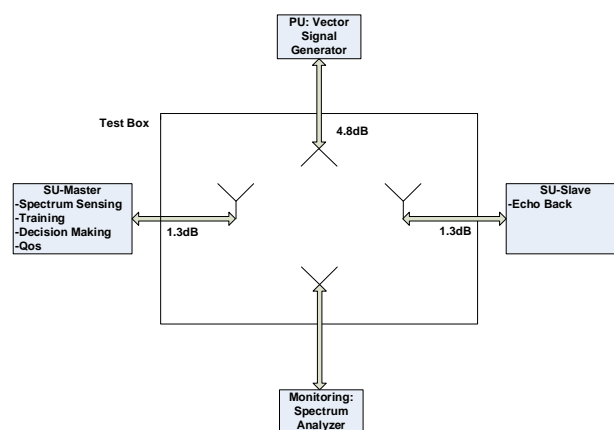


Figure 29: Test-bed implementation setup

The SUs are operating in a master-slave configuration each using the microcontroller TI MSP430 and the narrowband transceiver TI CC2500. The SU master and SU slave are connected to the antenna via coaxial cables (attenuation shown in Figure 29).

The SU master transmits data packets of fixed size and content while the SU slave returns the received data packets to acknowledge the correct reception without any packet repetition. The SU master determines the packet loss rate (PLR) as a measure of quality of service (QoS). Note that, a concept of packet repetition in case of packet loss decreases the PLR but increases the packet delay. Therefore analyzing the packet delay is an indirect metric and will not be analyzed. For each failure in receiving the correct acknowledgement, the SU master increases the number of packet losses. Further, the SU master performs spectrum sensing, prediction and decision making and informs the SU slave about the chosen communication channel.

The PU activity is generated by a vector signal generator (VSG). While the SUs are sensitive to the radio environment, the PU performs non-feedback cyclic data transmission.

8.3.1.1 Secondary User Setup

The SUs use two possible channels (CH1 and CH2). CH1 is the default channel which might be interfered by the PU. The second channel CH2 is the safe channel or the backup channel. Channel CH2 is only used if the predictive MAM determines a worse channel quality indication (CQI) for CH1. This simple scenario was selected in order to simplify the experiments.

The SU master transmits cyclic data packets. Initially, it uses the default channel CH1. Before each transmission the prediction methods determine the CQI of both channels CH1 and CH2. They are checked in order to tune to the best channel. The index of the best channel is transmitted as header field of the next data packet. In case, the SU slave receives the data packet without error than it acknowledges the reception with a data echo. Right after the transmission the slave tunes to the channel mentioned in the last data packet. In case the SU master receives the acknowledgment from the SU slave, it tunes also to the best predicted channel.

Table 6: SU test-bed features

Platform	CC2500 TRX- MSP430 μC	
Number of Channels	2	
Channel	CH1	CH2
Center frequency	2.45GHz	2.47GHz
Spectrum sensing	Energy detection (RSSI)	
Sample time	~ 90 μ s	
Frequency switching time	~ 100 μ s	
Traffic type	Cyclic	
Acknowledgment	Data Echo	
QoS	PLR in %	
Bit error detection	CRC-16	
Packet duration	~ 2.7ms	
Period	40ms	

Important features and selected time parameters for the SUs are summarized in Table 6.

8.3.1.2 Primary User Setup

Two selective IA scenarios are used based upon IEEE 802.11 PU activity. Important features and selected time parameters for the PU are summarized in Table 7.

Table 7: PU test-bed Parameters. A: high-load scenario, B: low-load scenario

Platform	Vector Signal Generator R&S
PU type	WLAN
Center frequency	2.45GHz
WLAN data packet duration	2ms
TX power	15dBm

PU antenna cable attenuation	4.8dB	
SU antenna cable attenuation	1.3dB	
Traffic type	Cyclic	
Scenario	A	B
Idle time	10ms	20ms
Duty cycle	20%	10%
Period	12ms	22ms

The PU is a single node transmitting data packets with a duration of 2ms.

8.3.1.3 Implementation

In total, four MAMs are implemented for evaluation: the predictive MAMs based on MM2, MM4, AR and a non-prediction (NP) MAM. In general, the methods proceed the following phases: training, prediction, and channel selection.

The NP MAM is the worst case method used as reference. This method constantly uses channel CH1 and has no ability to predict the PU activity or switch to channel CH2.

The MAMs based on MM2 and MM4 are based on the simple set of states $S = \{0,1\}$ to differ between idle and busy channel occupancy. In the training phase, five samples for each frequency channel i are observed. MM2 is only based upon the initial probability distribution. It uses the initial idle probability $\pi_{0,i} \in \Pi_i$ as channel quality indicator (CQI) for channel i :

$$CQI_{MM2}(i) = \pi_{0,i} \quad (52)$$

MM4 is based upon the idle and busy MM average distances $\bar{d}_{0,i}$ and $\bar{d}_{1,i}$ for channel i . Its difference is used as CQI for channel i :

$$CQI_{MM4}(i) = \bar{d}_{0,i} - \bar{d}_{1,i} \quad (53)$$

Finally in the channel selection phase, the MAMs determine the best channel based on the CQI. So, for the MAM k the channel $i = \operatorname{argmax}_i(CQI_k(i))$ with the highest CQI is selected as best channel.

The MAM based on AR works differently. The model generation has to be done based on a long observation sequence on the default channel CH1. The number of required samples was determined experimentally to 100 samples. Next, the model order and the model coefficients are determined as mentioned in Section 8.2.1. The processing is performed on a host computer using the numerical computing environment MATLAB. The model is then exported to the SU master. In the training phase, the default channel CH1 is observed for N samples, whereby N is the extracted model order. In the prediction phase, the future occupancy is predicted according Section 8.2.1. In total, N samples are predicted. During the channel selection phase, the presence of white space is analyzed. If the last 4 predicted samples will be idle, then the SU remains in the default channel CH1 otherwise the safe channel CH2 will be used in the next cycle.

Table 8: Medium access parameters

Predictive medium access	NP	MM2	MM4	AR
Training duration	No	10ms	10ms	15ms
Model order	No	1	1	15
Sample duration	No	1ms	1ms	1ms
CH1 samples	No	5	5	15
CH2 samples	No	5	5	0
Predictive type	No	Reactive	Reactive	Proactive
Model generation	No	Real-time	Real-time	Pre-processing
Prediction duration	No	33.8 μ s	120 μ s	3.83ms

Table 8 summarized the medium access parameters in our implementation. Further, the duration for the prediction processing is listed.

8.3.1.4 Implementation Validation

The cyclic SU data transmission using the predictive MAMs are illustrated in the measured spectrograms of Figure 30 to Figure 32. The measurement is done with the real-time spectrum analyzer Tektronix RSA6114A. The horizontal and vertical axis represent the frequency and the time, respectively.

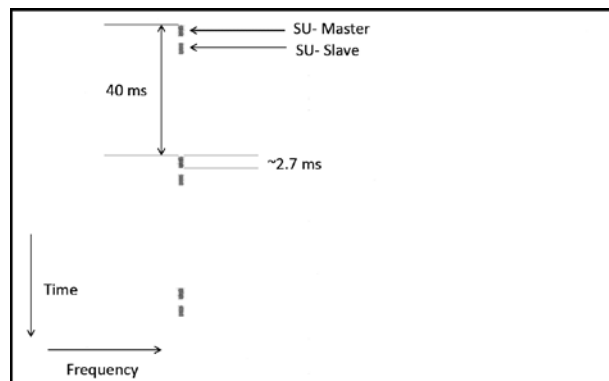


Figure 30: Spectrogram of master-slave data transmission in CH1 without PU inferences

The cyclic transmission period and the packet duration which are mentioned in Table 6, are illustrated in Figure 30 also. It shows the cyclic data packet transmission and acknowledgements in channel CH1 without PU activity.

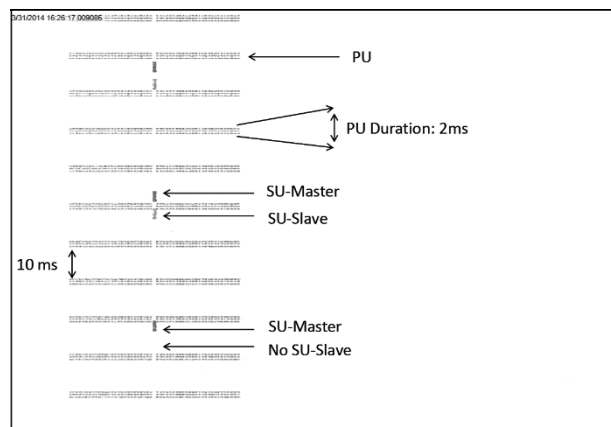


Figure 31: Spectrogram of master-slave data transmission with NP MAM in CH1 with PU interferences

The PU activity may interfere the data packet transmission and cause packet loss as shown in Figure 31. The SU slave does not receive the data packet and therefore does not transmit an acknowledgement. A predictive MAM bypasses PU future activity by switching to channel CH2 as shown in Figure 32.

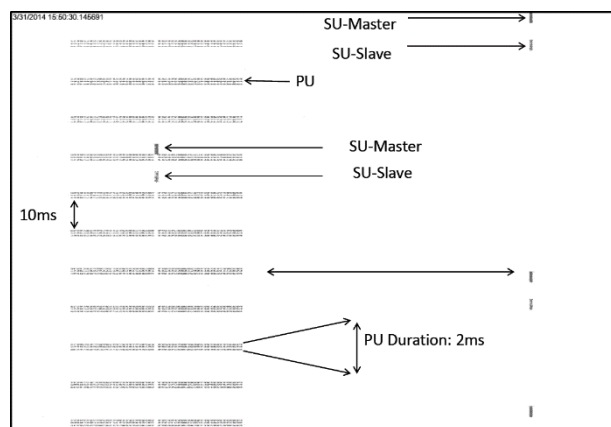


Figure 32: Spectrogram of master-slave data transmission with predictive MAM based on MM2. It switches to the safe channel CH2 in presence of the PU interferences in the default CH1

8.3.1.5 Results and Analysis

The MAMs are evaluated in both scenarios as mentioned above. Therefore, 1000 data packets are generated and transmitted for each test run. The tests runs are repeated 5 times to result in a representative evaluation. The PLR mean and standard deviation are listed in Table 9 and Table 10.

Table 9: PLR of predictive MAM tests in high-load scenario A

Medium access method	PLR mean	PLR standard deviation
NP	33.26%	0.114%
Based on MM2	0.46%	0.195%
Based on MM4	0.22%	0.045%
Based on AR	0.18%	0.071%

Table 10: PLR of predictive MAM tests in load-load scenario B

Medium access method	PLR mean	PLR standard deviation
NP	13.54%	0.195%
Based on MM2	0.36%	0.152%
Based on MM4	0.20%	0.099%
Based on AR	0.16%	0.055%

The average PLR without prediction (NP) in both load scenarios show the worst results as expected. Applying predictive MAMs decrease the PLR as can be seen in Table 9 and Table 10. Thereby, MAM based on AR has the lowest average PLR, which means it is the best prediction method. But it should be highlighted that the MAM based on AR needs to generate the model order and the model coefficients in a pre-processing phase. MM2 and MM4 result in a slightly higher average PLR than AR but they do not need any model generation and therefore are real-time capable.

It can be summarized that the MAM based on MM4 is the best compromise in prediction accuracy and real-time capability.

8.3.2 Experimental Investigation of Cooperative Medium Access

In Section 8.2.2 a cognitive method for cooperative medium access is introduced. This section discusses its experimental evaluation.

The introduced general ISAC concept is implemented and evaluated within an IA scenario. The specific ISAC network setup is shown in Figure 33.

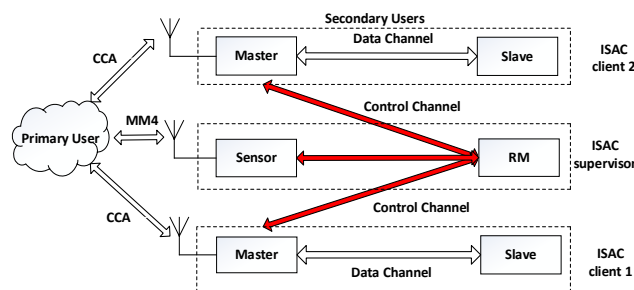


Figure 33. Measurement setup with interfering PU and SU containing an ISAC network with two ISAC clients

The master uses a frequency channel called data channel (DC) for data transmissions to its slave. Three frequency channels are available for data transmission. These three channels are named CH1, CH2, and CH3. These are the available spectral resources. Hence, the implementation is limited to spectral resources and does not consider the management of other resources such as temporal, code or spatial resources.

Another type of frequency channel is the dedicated CC, which is named CH0. For simplicity reasons, we assume that CH0 is not interfered by any primary user. In the following sections the SU and PU setups are discussed.

8.3.2.1 Secondary User Setup: ISAC Clients

In order to address a crowded IA scenario, we evaluate the ISAC network with two ISAC clients. Both ISAC clients are independent wireless systems performing real-time data transmission tasks. In order to lower the network implementation complexity, both ISAC clients are operating identically in a master-slave constellation, which is common in IA scenarios.

The master and slave are implemented in the microcontroller MSP430 of Texas Instruments (TI) with the narrowband transceiver CC2500. The master transmits data packets of fixed size and content while the slave returns the received data packets to acknowledge the correct reception. Important features and selected time parameters are summarized in Table I.

Table 11: SU ISAC client master and slave test-bed features

Platform	μ C MSP430 with transceiver CC2500			
Channel	CH0	CH1	CH2	CH3
Center frequency	2.43 GHz	2.44 GHz	2.45 GHz	2.46 GHz
Channel Type	CC	DC	DC	DC
Spectrum sensing	No	RSSI-based CCA prediction		
Sample time	-	~ 90 μ s		
Traffic	RARQ	Real-time data transmission		
Type	Event-based	Cyclic		
Period	-	40 ms		
Acknowledgment	-	Data echo		
QoS	No	PLR in %		
Packet duration	~1.2 ms	~2.7 ms		
Switching time	-	~ 100 μ s		
Bit error detection	-	CRC-16		

Each ISAC client starts communication on the default DC. The master is equipped with the sensing feature listen-before-talk by a clear channel assessment (CCA) based on the received signal strength indication (RSSI) within its current DC. In case of successful CCA the data transmission is continued in the current DC. Otherwise the current DC is interfered by the PU or the other ISAC client. As shown in Figure 34, before next data transmission, the master tunes to the CC in order to initiate a resource allocation negotiation. The ISAC supervisor response with the new allocated DC. After receiving the response from ISAC supervisor, the master tunes to the previous DC in order to notify the slave about the new allocated DC. The master tunes to the new allocated DC, when the slave successfully acknowledges (ACK) the notification. In case the notification is unsuccessfully acknowledged from slave, the master continues sending notification till receiving successful acknowledged from slave.

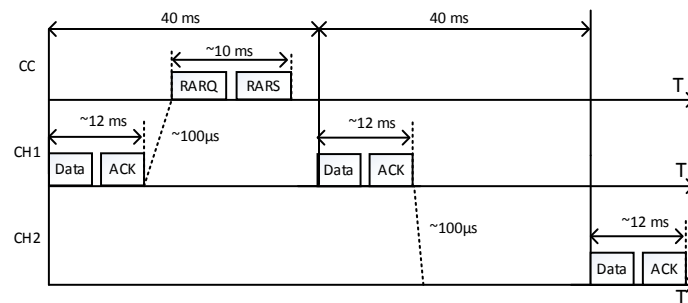


Figure 34. Timing diagram of master-slave resource allocation change within real-time data communication

The master does not stop data transmission during resource allocation negotiation. In case of resource allocation negotiation between master and supervisor failure, the master will tune to previous DC and will try to continue data transmission. With the next CCA failure, the master initiates a new resource allocation negotiation with ISAC supervisor. Therefore, the master does not lose any data transmission. The master performs the CC communication within its idle time. As a consequence, data transmission is always in real-time.

8.3.2.2 Secondary User Setup: ISAC Supervisor

The ISAC supervisor contains the sensor and the RM specified in Table II and Table III, respectively. The sensor and RM are also implemented in the microcontroller TI MSP430 with the narrowband transceiver TI CC2500.

Table 12: SU ISAC supervisor sensor test-bed features

Platform	μ C MSP430 with transceiver CC2500
Channel type	CC
Center frequency	2.43 GHz
Data packet duration	~ 1.2 ms
Bit error detection	CRC-16
Spectrum sensing	MM4-based DCs occupancy prediction
Acknowledgment	No
Traffic type	Cyclic
Idle time	30 ms
Duty cycle	~ 4 %
Period	~ 31.2 ms

The sensor senses all DCs periodically. Then, it determines two measures derived from the Markov model MM4 published in [51] and [43]. The first measure is the busy distance expressing the observed mean count of consecutive occupied samples within a certain DC, which are interfered by PUs. The second measure is the idle distance expressing the mean count of consecutive non-occupied samples, respectively. Based on the difference between the busy and idle distances, the DCs are sorted according to their quality. This information is given to the RM as DC quality indicators. Hence, the DC quality indicators provide information about the amount of interference of each DC.

Table 13: SU ISAC supervisor resource manager test-bed features

Platform	μC MSP430 with transceiver CC2500
Channel type	CC
Center frequency	2.43 GHz
Data packet duration	~1.2 ms
Bit error detection	CRC-16
Traffic	RARS
Type	Event-based

The RM has the responsibility to update the RAO. Therefore, it stores the very last DC quality indicators permanently. Hence, upcoming resource allocation decisions are based on the last stored DC quality indicators.

8.3.2.3 Primary User Setup

TABLE 14: PU TEST-BED FEATURES

Platform	Vector Signal Generator SMBV100A
PU type	Cyclic IEEE 802.11g-like transmission
Center frequency	2.45 GHz
Data packet duration	~2 ms
TX power	15 dBm
Traffic type	Cyclic
Idle time	10 ms
Duty cycle	~16.7 %
Period	~12 ms

A selected PU activity is based upon IEEE 802.11g-like transmissions, which is common in IA scenarios. The PU activity is generated by a vector signal generator. Further important features and selected time parameters for the PU are summarized in Table IV. While the SUs are sensitive to the radio environment, the PU performs cyclic data transmission without feedback from the radio environment based on CSMA/CA. The PU is a single device, which transmits data packets with a duration of 2 ms and a period of 12 ms. It is important to note, that only CH2 is interfered by the PU.

8.3.2.4 Implementation Validation

The cyclic SU and PU emissions using ISAC are illustrated in the measured spectrograms in Figure 35 and Figure 36. The measurements were done with the real-time spectrum analyzer Tektronix RSA6114A. The horizontal and vertical axis represent the frequency and the time, respectively. CH0 is CC and CH1, CH2 and CH3 are the defined DCs.

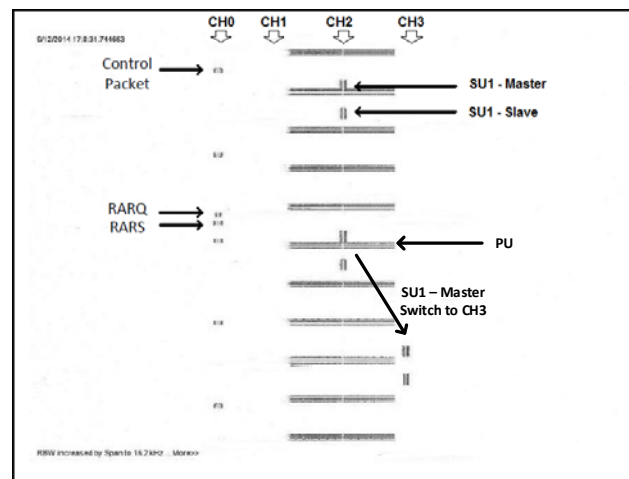


Figure 35. Spectrogram of the resource allocation negotiation with RARQ and RARS within the control channel of SU master and slave to avoid PU interference

The spectrogram ranges from 2.43 GHz to 2.48 GHz and has a duration of 100 ms.

Figure 35 shows the cyclic operation of the PU interfering CH2 where an ISAC client is transmitting data. This PU activity causes packet loss. The ISAC client detects PU activity and sends a RARQ to the RM. Then, according to RARS from the RM, the ISAC client tunes to the allocated free DC and therefore, bypasses future activity of the PU. In case of multiple ISAC clients, the RM allocates different DCs to each ISAC client while observing the PU interference.

As shown by the example in Figure 36, the PU interferes CH2 only while the ISAC clients transmit data in CH1 and CH3.

8.3.2.5 Results and Analysis

For evaluation, we measured the QoS within two different scenarios, which differ in the presence of PU interference. Within each scenario, we performed experiments for three different medium access types: Non-sensing (NS), non-cooperative (NC), and ISAC-based medium access. The implementation of the latter one was introduced in Section IV.

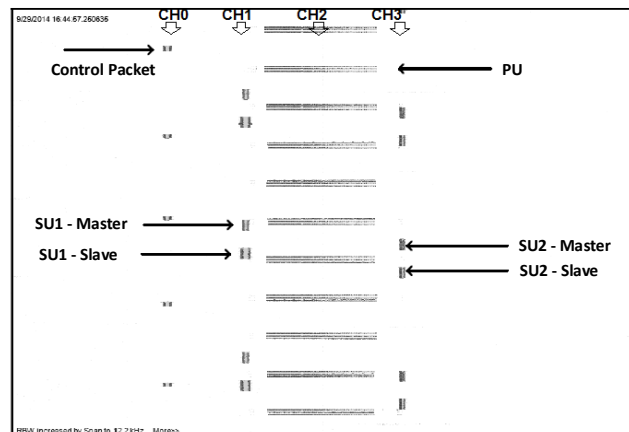


Figure 36. Spectrogram of two SU master-slave data transmissions within different frequency channels allocated by the resource manager

The NC medium access neglects the usage of the cooperative ISAC concept. I.e. each SU client works independently. In this setup, the master performs a CCA based on MM4 before each data transmission in the default DC CH2 as published in [51] and [43]. In case of CCA failure, the master switches to the backup DC CH3 after informing the slave. Hence, they try to omit the backup DC as much as possible.

The NS medium access even reduces the complexity of the non-cooperative medium access. The master does not sense the spectrum in terms of any CCA. Therefore, it is not able to predict spectrum occupancy or to detect PU interference. The master does not tune to any other channel either. Hence, there will be data transmission collisions and packet loss. The experiments are performed with a measurement duration for 1000 data packet transmissions, which are repeated 5 times and are averaged to result in a representative evaluation. Thereby, the master of both real-time wireless systems for each experiment determines the packet loss rate (PLR) as a measure of QoS. For each failure in receiving the correct ACK, the master increase the number of packet losses. Figure 37 and Figure 38 show the result of all experiments in case of PU interference absence and presence, respectively. The horizontal and vertical axis represent the medium access types in different devices and the PLR, respectively in Figure 37 and Figure 38.

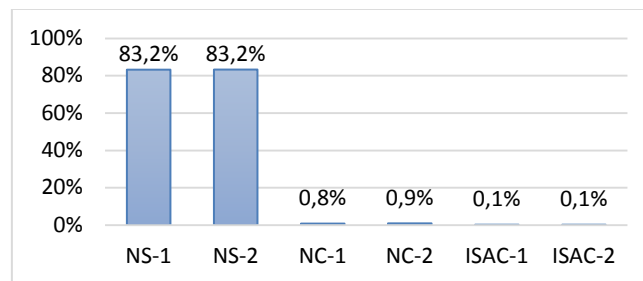


Figure 37. PLR (vertical axis) of two master-slave constellations (index 1 and 2) for the medium access methods (horizontal axis) non-sensing (NS), non-cooperative (NC) and ISAC in absence of PU

They show the PLRs for both real-time wireless systems. Clearly, NS medium access has the worst performance in both scenarios. This results from its non-cooperative and non-adaptive

medium access. In case of no PU interference, the two real-time wireless systems interfere each other.

The same disturbance can be observed also for the NC medium access but the PLR is below one percent without PU activity. The NC medium access avoids the PU interference much better than the NS medium access. However, the PLR is above 25% with PU activity.

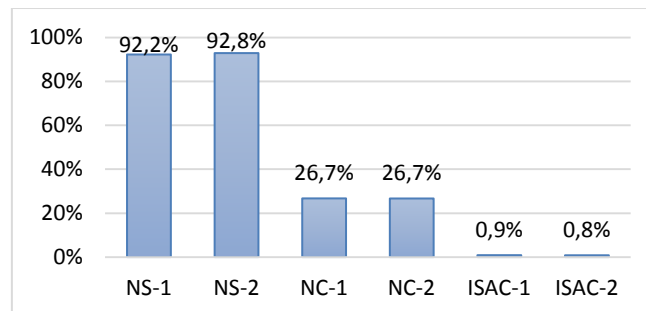


Figure 38. PLR (vertical axis) of two master-slave constellations (index 1 and 2) for the medium access methods (horizontal axis) non-sensing (NS), non-cooperative (NC) and ISAC in presence of PU

The best performance can be seen for the ISAC-based medium access. The PLR is below one percent even in presence of PU interference.

8.3.3 Experimental Investigation of Interference Signal Classification

In Section 8.2.3 a cognitive method for interference signal classification approach is introduced. This section discusses its experimental evaluation.

A specific measurement setup was prepared to put the NFSC approach to the test, as outlined in Figure 39.

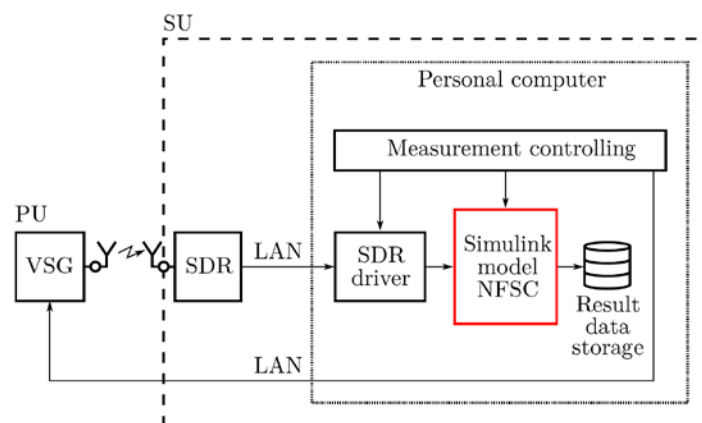


Figure 39: Measurement setup

8.3.3.1 Measurement Setup

The measurement setup is composed of the following components, which are discussed next in detail.

1. A PU system and a
2. SU system, whereas the latter one consists of:

- a) A SDR, a
- b) measurement controlling element, a
- c) SDR driver, a
- d) Simulink model of the NFSC approach, and a
- e) result data storage, whereas the last four components are within a personal computer.

As a last point, some significant measurement parameters are discussed at the end of this section.



Figure 40: Rohde & Schwarz SMBV100A vector signal generator

The PU system acts as a stimuli for the being tested SU system and is generated by a vector signal generator (VSG). A VSG is a signal generator that is capable of generating modulated complex radio signals and it typically provides a large number of various modulation formats. In addition, many VSGs can generate complex radio signals of digital communication systems that are based on well-defined standards, such as the standard wireless technologies (SWTs) IEEE 802.11 network standard family and Bluetooth. In this thesis, the VSG SMBV100A from Rohde & Schwarz was deployed, as shown in Figure 40, to generate complex radio signals of the standards IEEE 802.11g and Bluetooth. More precisely, PU signals are generated by the VSG via its sophisticated built-in arbitrary waveform generator by employing pre-configured waveform files. Waveform files are beforehand created on a personal computer with Rohde & Schwarz's ARB Toolbox PLUS software. The applied PU system signals are more discussed later.

The SU system is the to being tested component of the measurement setup. It can be seen as two parts, a high frequency part and a baseband part, where the former one provides a wireless connection of the SU system to the measurement environment and the latter one does all other processing. The high frequency part contains only one component, a SDR, whereas the baseband part consists of four elements within a personal computer: 1) A measurement controlling element, 2) a SDR driver, 3) a Simulink model of the NFSC approach, 4) and a result data storage. Both SU parts are linked together by a Gigabit Ethernet connection.



Figure 41: Ettus Research USRP N210 software defined radio

The SDR, as written above, acts as a wideband receiver of the SU system for PU signals. The SDR USRP N210 from Ettus Research was deployed, as presented in Figure 41.

The measurement controlling element is in control of the entire measurement process and parameterizes the SDR driver, the Simulink model, and the VSG, before a measurement is conducted. Furthermore, it links the SDR with the Simulink model of the NFSC approach over the SDR driver, whereas the Simulink model stores its measured data in the result data storage. The VSG is also operated by means of remote control commands via a LAN connection. MathWorks MATLAB 2014a is the applied software for measurement controlling. Moreover, several scripts and functions were written in MATLAB language by the author of this thesis, which forge the measurement controlling element.

The SDR driver is a hardware driver provided by the manufacturer of the SDR. It enables a data connection of the SDR with the Simulink model. The USRP Hardware Driver (UHD) version 003.005.001 from Ettus Research was deployed.

The device under test is the NFSC approach, which was implemented in a Simulink model. Simulink is a data flow graphical programming language tool from MathWorks for modeling, simulating, and analyzing multi-domain dynamic systems. The Simulink model runs on the Rapid Accelerator mode, which enables a high acceleration of its performance. In detail, from the implemented Simulink model a standalone executable program is generated, which runs as a single process inside the personal computer during the measurement.

Conclusive, the measured data from the NFSC are stored during each measurement run on the hard drive disk of the personal computer.

All measurements were conducted without any other wireless transmitters present in the applied 2.4-GHz-ISM radio band and under constant measurement parameters, where notable ones are summarized in table 4.1.

Table 15: Measurement parameters

Parameter	Symbol	Value
Center frequency	f_{SDR}^0	2.423 GHz
Display bandwidth	B^{DI}	10 MHz
Resolution bandwidth	Δf	39.22 kHz

The center frequency f_{SDR}^0 of the SDR was set to the right edge of the channel bandwidth of the first IEEE 802.11g frequency channel $f_{802.11g,1}^0 = 2.412 \text{ GHz}$, as diagrammed in Figure 42.

8.3.3.2 Simulink Model

In Simulink, dynamic systems are graphically modeled as block diagrams. A block diagram can consist of layers, where each layer is defined by a subsystem. Within a block diagram, a system is described by blocks and lines. Blocks are used to generate, modify, combine, and output signals, whereas lines are used to transfer signals from one block to another. The transfer of signals between blocks is realized over input and output terminals. A signal can

be either a scalar signal or a vector signal. Furthermore, a variety of various blocks is provided by Simulink, whereby user-defined blocks can also be created as a subsystem.

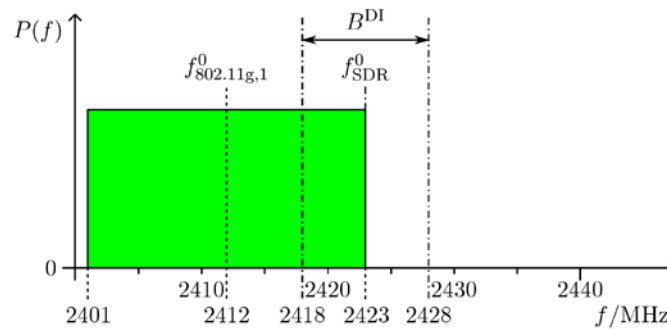


Figure 42: Measurement parameters

The NFSC approach was implemented in a Simulink block diagram with six subsystems, one for each layer of the NFSC approach, compare Figure 19. Each of this six subsystems is an enabled subsystem, whereby one subsystem is highlighted in Figure 43. An enabled subsystem is only executed when the signal driving the subsystem enable port is greater than zero.

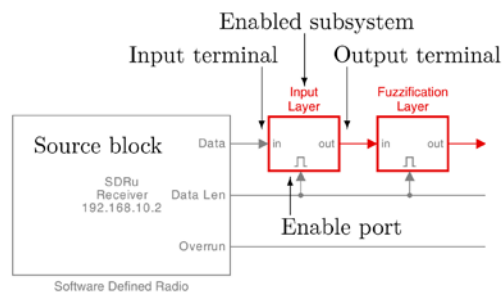


Figure 43: Block diagram with an enabled subsystem

In concrete terms, the SDR driver provides a Simulink source block of the SDR, which outputs the acquired complex samples of a received PU signal.

Since the SDR is connected with the personal computer via a Gigabyte Ethernet connection, acquired samples are transferred from the SDR to the personal computer within an Ethernet frame. The number of samples per Ethernet frame is set to the default value of 362, which optimally utilizes the underlying Ethernet payloads for a standard 1500-byte maximum transmission unit. Whenever a new Ethernet frame is received by the source block from the SDR, all complex samples within this Ethernet frame are provided as a scalar signal at the *Data* port of the source block. Furthermore, a trigger signal greater than zero is generated at the same time on the *Data Len* port, indicating that a new Ethernet frame is received. The trigger signal is connected to all aforementioned six subsystems and enables them, when a new Ethernet frame is received.

Since the SDR transfers its samples to the Simulink model in an Ethernet frame, the processing of the samples within Simulink can also be performed in a frame-based matter. Signals in Simulink can be either sample- or frame-based signals. Frame-based signals within

Simulink maximizes the efficiency of the model by processing multiple samples at once. A frame-based signal is created from a sample-based signal by the frame conversion block, see Figure 44. Being specific, the generated scalar signal from the source block is transferred into a Simulink frame as a (362×1) vector signal by the frame conversion block within the input layer, compare Figure 20. The vector signal, expressed in other words, is a two dimensional matrix.

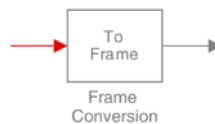


Figure 44: Frame conversion block

The frame conversion block in the input layer is followed by two blocks: Data type conversion block and normalization block, as highlighted in Figure 45. Depending on the selected output data type of the SDR, a data type conversion is required, because the FFT block requests a float data type on its input. The SDR provides three output data types: int16, single, and double. A output data type of int16 was selected, because it requires less bits per sample and it, therefore, enables a higher throughput of samples over the Gigabyte Ethernet connection between the SDR and the Simulink model. The subsequent normalization block, with a gain of $\frac{1}{2^{15}}$, is optionally added.

It maps the acquired int16 samples within interval $[2^{15}, 2^{15} - 1)$, after the conversion into a float data type, to the interval of $[-1, 1)$.

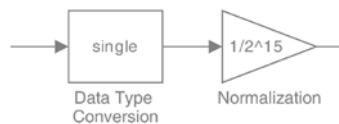


Figure 45: Data type conversion and normalization

The frame size of the (362×1) vector signal is changed next within the FFT block, depending on the selected FFT length. The applied FFT length is 256, which results from the selected measurement parameters, compare table 4.1 and eq. (3.6). Therefore, the output signal of the FFT block is a (256×1) vector signal.

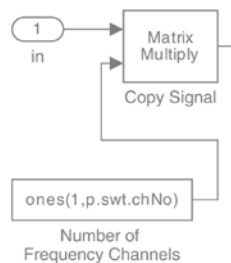


Figure 46: Copy signal

After fuzzification, this (256×1) vector signal is extended within the filtering layer, as highlighted in Figure 46. In detail, the vector signal is extended with its copy n times, depending on the number of frequency channels n of the to be classified SWT. For IEEE

802.11g, the vector signal is extended to (256×13) , whereas for Bluetooth to (256×79) . This n -times duplication of the PSD is added, so that the filtering within the filtering layer is actually only a simple matrix multiply, compare Figure 23. This improves the performance of the model, since MATLAB or Simulink is specialized for matrix operations.

8.3.3.3 Industrial Environment Scenarios

The evaluation of the NFSC is realized with the aid of six selected heterogeneous and harsh ISs. An IS consists of a PU system and a SU system in a bounded environment, where the data transmission of the PU system interfere the data transmission of the SU system, as depicted in Figure 47.

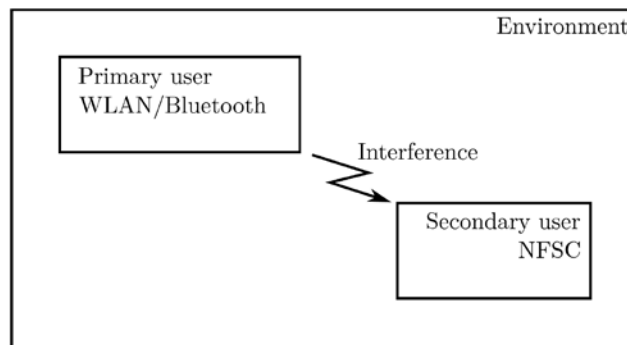


Figure 47: Bounded environment of an industrial scenario

A PU system is a data transmission between several wireless nodes on the basis of one or two SWTs, like IEEE 802.11 network standard family, such as WLAN; and/or Bluetooth. The NFSC acts as the SU system and its classification performance of PU systems is put to the test in this evaluation.

An IS depends on two parameters. Firstly, on the selected SWT, like WLAN, Bluetooth or a combination of both. Secondly, on the chosen medium occupancy (MO) for a SWT:

$$MO = \frac{t_{on}}{t_{on} + t_{off}} \quad (54)$$

where MO is the ratio of active transmission time t_{on} of the SWT to the sum of active transmission time and inactive transmission time t_{off} of the same SWT.

Since this thesis focuses on classification of 2.4-GHz-ISM radio band SWTs in an industrial environment, two SWTs are chosen as an example for PU systems. It is assumed that an industrial automation is equipped with a WLAN as a base infrastructure such as LAN. On the other hand, Bluetooth is used as a PAN at electrical machines, such as for transmitting sensor data of an industrial robot. Industrial robots often have many rotational axes, like the human arm, which makes it difficult using a wired communication for sensor's data transmission of the robot.

For the NFSC evaluation two different MOs are chosen for a SWT: high load (HL) and low load (LL). HL is a maximum data transmission throughput of a SWT, whereas LL is a minimum data transmission throughput. An overview of the utilized ISs in this evaluation is presented

in table 5.1. First, each SWT is evaluated by its own with both MO extremes. Next, two combinations of both SWTs are used for evaluation.

Table 16: Overview of industrial scenarios

Industrial Scenario	WLAN HL	WLAN LL	Bluetooth HL	Bluetooth LL
IS1	Yes	-	-	-
IS2	-	Yes	-	-
IS3	-	-	Yes	-
IS4	-	-	-	Yes
IS5	Yes	-	Yes	-
IS6	-	Yes	-	Yes

For WLAN, IEEE 802.11g is chosen. Reason is, it has the shortest symbol duration time of the IEEE 802.11 network standard family in the 2.4-GHz-ISM radio band. The shorter the symbol duration time, the more difficult it is for the NFSC to recognize transmitted packets of the PU system, leading to a more critical performance evaluation of the NFSC. Further, the first frequency channel is chosen with a center frequency f_c of 2412 MHz.

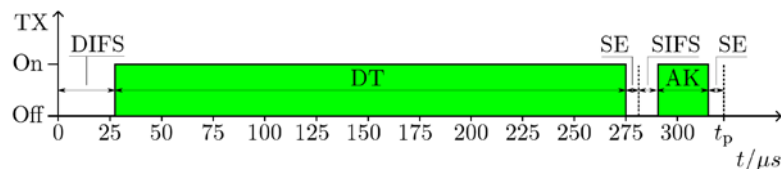


Figure 48: Transmission timings of industrial scenario WLAN high load

The MO of WLAN HL derives from a scenario of one access point and a great number of clients. All clients are continuously transmitting data frames to the access point and being acknowledged by the access point. With an infinite number of clients the probability is 100% that there will be always a client that picks the first slot time of the contention window. Therefore, the contention window can be neglected. The WLAN HL transmission timings are depicted in Figure 48. The client's data (DT) frame is drawn as DT and the access point's acknowledgement (AK) is AK, where transmission occurs. During DCF interframe space (DIFS), signal extension (SE) and short interframe space (SIFS) no transmission occurs. This transmission sequence is repeated with the period of t_p . The MO of WLAN HL is $MO_{WLAN,HL} = 84.47\%$.

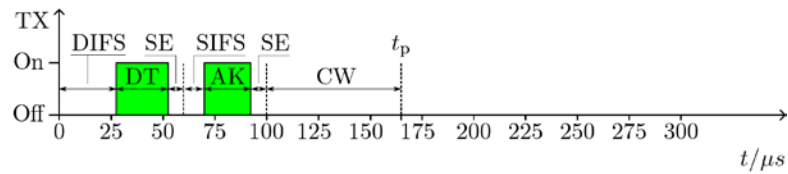


Figure 49: Transmission timings of industrial scenario WLAN low load

The MO of WLAN LL derives from a scenario of one access point with a single client. The client is also continuously transmitting data frames to the access point and being acknowledged by the access point. With only one client the contention window can be assumed as 7.5 slot times, the average of the minimum contention window of 15 slot times. The LL transmission timings are depicted in Figure 49. The MO of WLAN LL is $MO_{WLAN,LL} = 30.68\%$.

For Bluetooth all non-occupied frequency channels are used. So, in IS3 and IS4 all 79 frequency channels are used. But in IS5 and IS6 Bluetooth is interfered by WLAN in its first channel, therefore the first 22 frequency channels are occupied and blocked for Bluetooth communication.

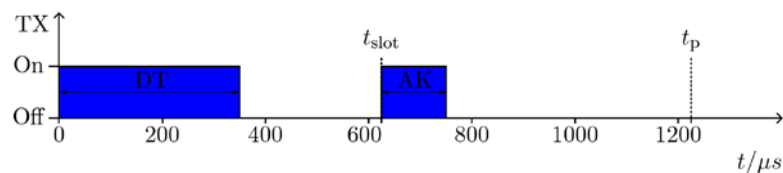


Figure 50: Transmission timings of industrial scenario Bluetooth high load

The MO of Bluetooth HL derives from a scenario of two Bluetooth nodes. Each node is continuously transmitting data frames to the other node and being acknowledged by the latter one. The corresponding transmission timings are depicted in Figure 50. The data frame DT contains the maximum payload. The MO of Bluetooth HL is $MO_{Bluetooth,HL} = 39.36\%$.

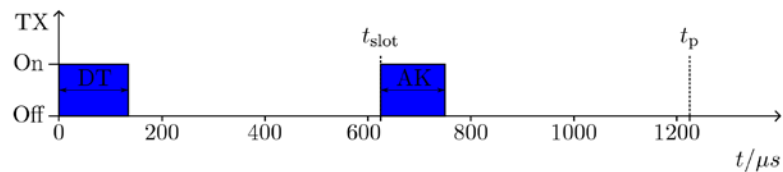


Figure 51: Transmission timings of industrial scenario Bluetooth low load

The MO of Bluetooth LL derives from the same scenario with two Bluetooth nodes. But the data frame DT contains the minimum payload. The corresponding transmission timings are depicted in Figure 51. The MO of Bluetooth LL is $MO_{Bluetooth,LL} = 20.80\%$.

8.3.3.4 Results and Analysis

The classification performance of the NFSC is evaluated through the two statistical measures: sensitivity and specificity. Following a detailed description is given of the procedure of obtaining these statistical measures.

First of all, although the NFSC's last two layers are proposed in [50] for distinguishing between a hopping and a non-hopping PU system, the evaluation of the NFSC is carried out directly through the also recorded SMs.

The SMs for all corresponding PU frequency channels were recorded for a measurement duration of 11 s, as shown for an arbitrary frequency channel in Figure 52. The complete measurement run is next divided into two parts: a transition area followed by a measuring window.

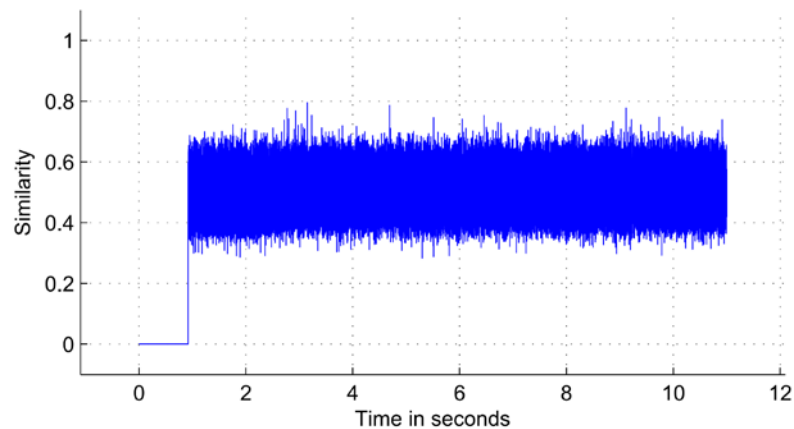


Figure 52: Complete measurement run of an arbitrary frequency channel

In the beginning of the transition area is the SM value for almost one second zero. The reason for this is, that some time is required for establishing the connection between the single NFSC process of the Simulink model inside the personal computer and the SDR. Next, some short time is required until the NFSC is in steady-state.

The subsequent applied measuring window is presented in Figure 53 and its duration is chosen to ten seconds. As the duration of the measuring window is substantial longer than the duration of each IS, a statistical analysis of the SM's data distribution is followed.

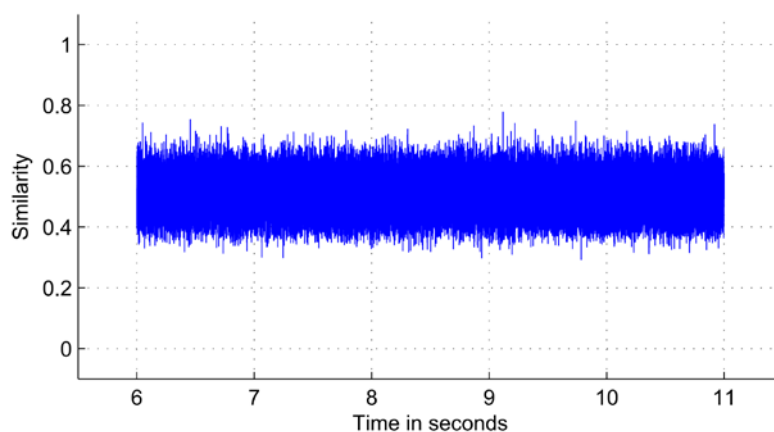


Figure 53: Measuring window of an arbitrary frequency channel

As a first step of the statistical analysis, a normalized frequency distribution, also known as empirical probability, is computed from the SMs, depicted as a histogram in Figure 54. All histograms were created with 100 bins for the similarity interval from zero to one.

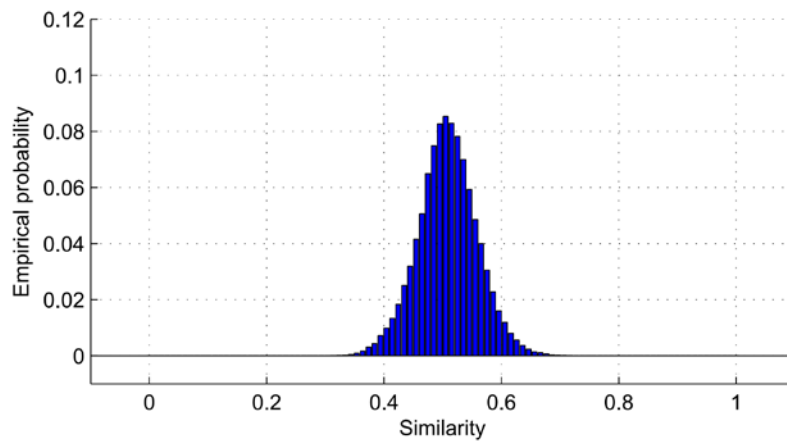


Figure 54: Histogram of an arbitrary frequency channel

As the second step, all histograms from all recorded frequency channels are compared with each other, plotted as an error bar with mean value and standard deviation in Figure 55. This figure shows exemplarily the IS1 with WLAN HL, where the PU system is transmitting on frequency channel one. A high similarity is measured on channel one, whereby a low similarity is measured on channel six. The former one corresponds to the transmitting PU system and the latter one is resulting from noise. In between those two channels is a moderate similarity measured, but no PU system is present on these channels. This issue arises from the overlapping channels of the IEEE 802.11g network standard. Specific, the PU system on channel one overlaps with the channels two till five.

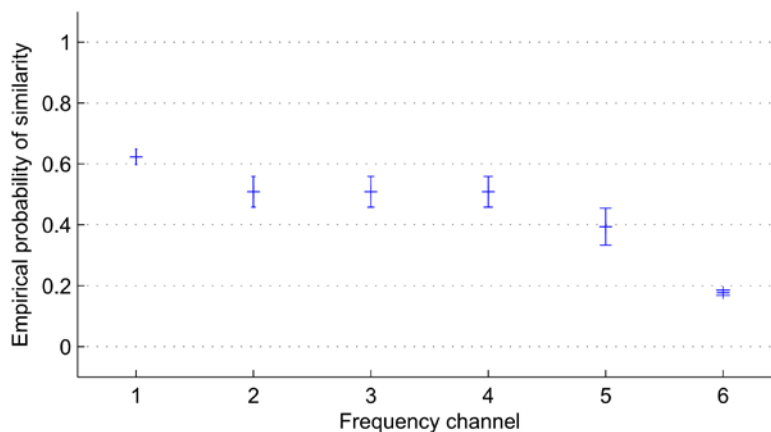


Figure 55: Error bar of several frequency channels

Sensitivity and specificity are a statistical measures of the performance of a binary classification test. Sensitivity and specificity measure the proportion of correctly identified actual positives and negatives, respectively.

In general, positive = identified and negative = rejected. Therefore:

- TP = correctly identified
- FP = incorrectly identified
- TN = correctly rejected
- FN = incorrectly rejected

The four outcomes can be formulated in a 2×2 confusion matrix, as shown in Table 17.

Table 17: Confusion matrix for primary user systems

		Detected class	
		Positive PU	Negative Noise
Actual class	Positive PU	TP PU actually present	FN PU not detected
	Negative Noise	FP PU wrongly detected	TN PU actually absent

With this, sensitivity TPR is defined as:

$$TPR = \frac{TP}{TP + FN} \quad (55)$$

where it is also known as true positive rate.

Further, specificity TNR is defined as:

$$TNR = \frac{TN}{TN + FP} \quad (56)$$

where it is also known as true negative rate.

The outcome of the evaluations are shown in Figure 56 to Figure 59.

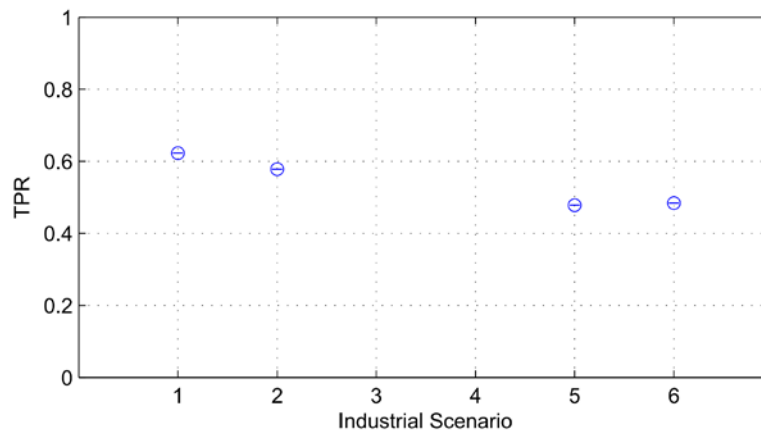


Figure 56: Sensitivity of all industrial scenarios classified as WLAN

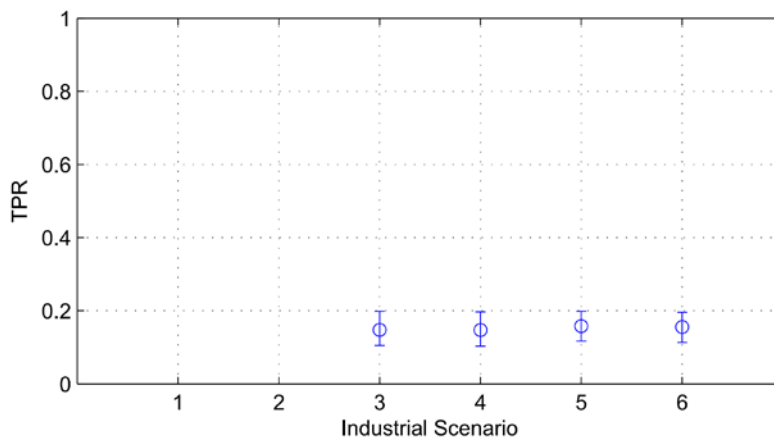


Figure 57: Sensitivity of all industrial scenarios classified as Bluetooth

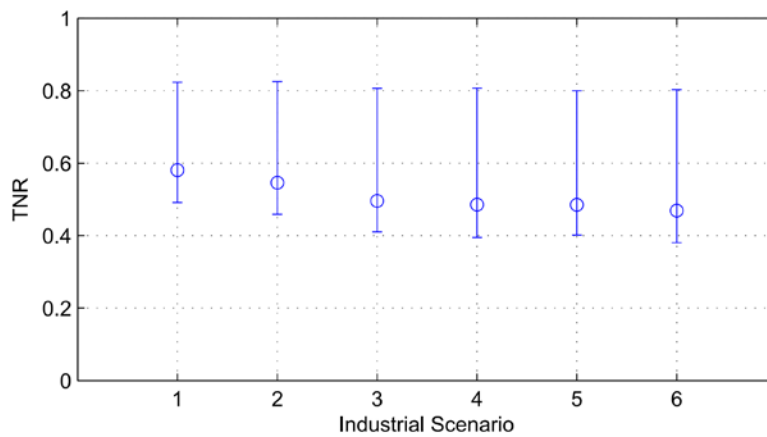


Figure 58: Specificity of all industrial scenarios classified as WLAN

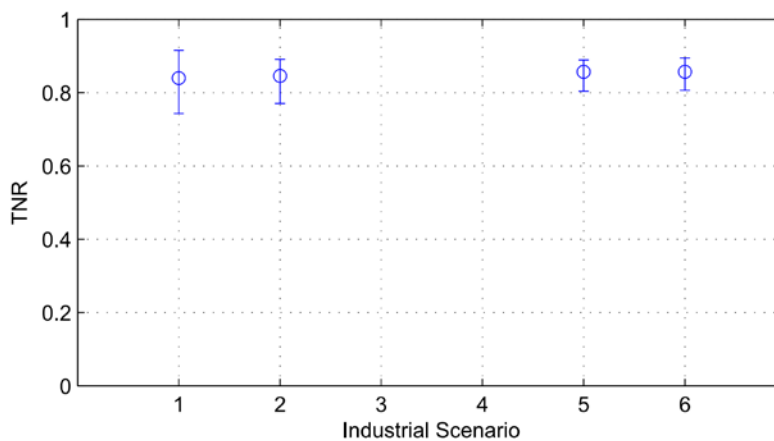


Figure 59: Specificity of all industrial scenarios classified as Bluetooth

Sensitivity is low throughout all ISs, while specificity was measured in general high. Averagely, WLAN was detected with a moderate rate of 55% and Bluetooth only with 15%. On the contrary, a typical specificity of 50% were measured. For Bluetooth even up to 90%.

Concluding the results, absent PU systems are getting better detected by the NFSC as present ones. In other words, nothing to find is easier than finding something. NFSC's scope

of application is, therefore, rather detecting free gaps in its radio resources than identifying PU systems by their utilized SWT.

8.4 Recommendations for Cognitive Methods

In the previous section the results of the performance evaluation of the cognitive methods are presented. Based on its conclusions future design of wireless medium access methods can be advised. Such recommendations are heavily dependent on implementation aspects. While some wireless technologies appreciate high-power computation and wideband radio frequency frontends others prefer low power narrowband radio frequency frontends.

In the following Section 8.4.1, major implementation aspects are introduced. Based on the implementation aspects, the subsequent Section 8.4.2 derives cognitive method recommendations.

8.4.1 Implementation Aspects

The limiting implementation aspects are mainly the medium access type and radio frequency frontend hardware constraints.

8.4.1.1 Autonomous and Cooperative Medium Access

A wireless medium access method design may appreciate an autonomous medium access without any central medium access management. Such requirements are appropriate for low-power low-rate building and process automation applications but also for fast-varying ad hoc networks e.g. car-to-car communication applications.

But many wireless technologies prefer centralized cooperative medium access. It enables deterministic and efficient medium usage requiring fixed and accessible central radio devices. Typical applications are static communication networks for building, process and factory automation. Next to automation applications, home and office communication infrastructures benefit from central medium access management because of its simplicity. Also mobile networks deploy a cell-based central medium access.

8.4.1.2 Dedicated and Combined Spectrum Sensing Frontend

The choice of cognitive methods depends heavily on the availability of an additional radio frequency frontend dedicated to spectrum sensing. It enables continuous spectrum sensing and therefore enhances interference awareness. But an additional dedicated spectrum sensing frontend requires additional hardware components and increases the total power consumption.

Otherwise the combined spectrum sensing frontend has to cope with both demands: communication and spectrum sensing. Consequently, it decreases the spectrum sensing accuracy. So, it targets especially low-power applications.

8.4.1.3 Wideband and Narrowband Spectrum Sensing Frontend

The choice of cognitive methods depends also heavily on spectrum sensing frontend constraints. The major spectrum sensing frontend feature is its input bandwidth. Frontends with an input bandwidth greater or equal to the spectrum band of interest are called wideband frontends. Wideband signal processing requires additional computational power e.g. a dedicated DSP-unit and consumes a lot of power.

The low-power approach is a narrowband spectrum sensing frontend. But it lacks of information loss due to its sequential approach for spectrum sensing. This results in less accurate classification and prediction results.

8.4.2 Cognitive Methods Recommendations

Based on the cognitive methods introduced in Section 8.2 and evaluated in Section 8.3 future design of wireless medium access methods can be advised. The recommendations can be categorized into the tasks:

1. Resource assessment
2. Resource allocation

The term resources refers to the hyperspace introduced in [47] consisting of multiple dimensions such as spectrum, time, code and the spatial dimension as discussed in Section 8.2.2. The recommendations for cognitive methods are limited to spectral and temporal resources. Spectral and temporal resources are flexible in the utilization and do not require costly additional hardware components because most standard wireless transceiver permit additional latencies and also limited variation in frequency usually in terms of finite frequency channels.

The first task of resource assessment refers to an evaluation process of the usable resources. It includes resource sensing and occupancy prediction. The second task of resource allocation refers to the decision process to utilize the available resources in an efficient way.

The following sub-sections list the recommended cognitive methods of both tasks for the spectral and temporal resource, respectively.

8.4.2.1 Spectral Resource Assessment

Interference awareness assumes solid knowledge about non-cooperative interfering systems. Especially, if industrial applications require reliability and a deterministic medium access. Therefore, we recommend NFSC-based interference signal classification for spectral resource assessment.

The input of the NFSC model is the measured PSD. The PSD can be computed via sequential spectral sampling in case of a narrowband spectrum sensing frontend. In case of a wideband spectrum sensing frontend, the PSD can be computed with a FFT. Finally, the recommendation for efficient spectral resource assessment can be concluded:

Spectral resource assessment shall be performed with the NFSC interference signal classification with an incoming PSD based upon sequential spectral sampling in case of narrowband spectrum sensing frontend or in case of wideband spectrum sensing frontend the PSD is based upon FFT computation.

8.4.2.2 Spectral Resource Allocation

The spectral resource assessment recommendation depends only on the constraints of spectrum sensing frontends. Thereby, the spectrum resource allocation addresses mainly the medium access type. In case of autonomous medium access, only autonomous spectral

resource allocation is possible. Otherwise, we recommend ISAC-based cooperative spectral resource allocation.

Further, the approach depends on the availability of an additional radio frequency frontend. In case of a combined spectrum sensing frontend with no additional radio frequency frontend, we recommend a reactive approach for spectral resource assessments. In the ideal case of a dedicated spectrum sensing frontend, we recommend a parallel continuous proactive approach for spectral resource assessments, which removes additional latency for spectrum resource assessment and allows to start the decision process immediately.

The recommendation for efficient spectral resource allocation can be summarized:

Spectral resource allocation shall be performed autonomously in case of autonomous medium access and otherwise cooperatively based on ISAC. In both cases the spectral resource assessments shall be performed proactively with a dedicated spectrum sensing frontend and reactively with a combined spectrum sensing frontend.

8.4.2.3 Temporal Resource Assessment

The temporal resource assessment recommendation orientate on challenging real time requirements of industrial applications. Therefore, we recommend the fast assessment based upon MM4. It is based on a temporal binary occupancy observation sequence determined from energy detection derived from the consecutive RSSI values.

An exception is the case of autonomous medium access with wideband spectrum sensing frontend. We recommend to extract the temporal binary occupancy observation sequence from the spectral resource assessment. The multiple usage of the outcome reduces the computational complexity and latency.

The recommendation for efficient temporal resource assessment can be summarized:

Temporal resource assessment shall be performed based upon MM4 whereby the incoming binary occupancy sequence is concluded by RSSI measurements. In case of autonomous medium access with wideband spectrum sensing frontend the sequence shall be extracted from the spectral resource assessment.

8.4.2.4 Temporal Resource Allocation

We recommend an autonomous temporal resource allocation. A cooperative resource allocation increases the latency and is therefore not capable for challenging real-time industrial applications.

Further, we recommend reactive temporal resource allocation in case of combined spectrum sensing frontend, which increases the latency. In the ideal case of a dedicated spectrum sensing frontend, we recommend proactive temporal resource allocation without any delay.

The recommendation for efficient temporal resource allocation can be summarized:

Temporal resource allocation shall be performed in an autonomous reactive way in case of combined spectrum sensing frontend, and in an autonomous proactive way in case of dedicated spectrum sensing frontend.

8.5 Conclusion and Future Work

The research project KOSYS discusses coexistence issues of wireless MAMs with focus on the license-free 2.4 GHz ISM radio band which is shared by numerous wireless technologies.

Firstly, we showed the performance limitations of non-adaptive and adaptive MAMs. We discussed the limitations of state-of-the-art standard wireless technologies such as IEEE 802.15.4 and its derived technology WirelessHART, IEEE 802.11 and also Bluetooth. We also simulated a non-adaptive and an adaptive MAM in worst-case dense industrial scenarios. The final results are twofold. While the adaptive MAM performance is closer to the industrial requirement of negligible PLR, the non-adaptive MAM reaches the industrial requirement of a deterministic transmission time, easily. But both MAMs do not achieve both requirements.

Additionally, we introduced novel cognitive methods to face the limitations of non-adaptive and adaptive MAMs. We introduced three cognitive methods for autonomous MAMs: Two based on Markov model (MM2 and MM4) and one based on auto-regressive model (AR). They predict the binary frequency channel occupancy based on observations.

Further, we proposed a novel cooperative MAM called inter-system automatic configuration MAM (ISAC MAM). The approach is operating in-between wireless systems such as IEEE 802.11, WirelessHART and Bluetooth, which is called ISAC network. Thereby, the design of ISAC has mainly the goal of interference awareness, to ensure real-time and reliable communication, and finally investment protection for existing wireless systems for easy adoption for wireless technologies manufactures.

Finally, we propose a cognitive method for interference awareness called neuro-fuzzy signal classifier (NFSC). It utilize a-priori known signal features such as bandwidth and center frequency to classify PU systems by applying fuzzy logic based rules.

The performance of cognitive methods were evaluated and analyzed. Therefore all introduced and proposed cognitive methods were implemented and extensive measurements in harsh industrial scenarios were performed.

The three cognitive methods for autonomous MAMs based on MM2, MM4 and AR were evaluated in a selected worst-case industrial scenario. They were implemented in a narrowband master-slave-constellation network with wideband IEEE 802.11 interference. Thereby, the MAM based on AR has the lowest average PLR, which means it is the best prediction method. But it should be highlighted that the MAM based on AR needs to generate the model order and the model coefficients in a pre-processing phase. MM2 and MM4 result in a slightly higher average PLR than AR but they do not need any model generation and therefore are real-time capable. It can be summarized that the autonomous MAM based on MM4 is the best compromise in prediction accuracy and real-time capability.

Further, we evaluated the cognitive method ISAC MAM for cooperative medium access in a worst-case industrial scenario. Two independent narrowband wireless systems were implemented which are interfered by wideband IEEE 802.11 communication. In case of no cooperation between the two wireless systems the PLR is above 25% in presence of

interference. The best performance can be seen for the ISAC-based MAM. The PLR is below one percent even in presence of PU interference.

Finally, we evaluated the cognitive interference signal classification method NFSC within six industrial scenarios with wireless systems IEEE 802.11 and Bluetooth. A wideband SDR was used as radio-frequency frontend for the MATLAB implementation. The proportion of correctly identified actual interfering signals is low throughout all industrial scenarios. Averagely, IEEE 802.11 was detected with a moderate rate of 55 % and Bluetooth only with 15 %. In contrast, the proportion of correctly identified actual absent signals was measured in general high. Typical values of 50 % were measured, which rise for Bluetooth even up to 90 %. Absent interfering wireless systems are better detected by the NFSC approach as present ones. Therefore, NFSC's scope of application is rather detecting free gaps in its radio resources than identifying interfering wireless systems.

From the evaluation performance, we derived general recommendations for future designs of cognitive MAMs based on medium access type and radio frequency frontend hardware constraints. Thereby, the spectral resource assessment is recommended to be performed with the NFSC based on wideband spectrum sensing. Further, the spectral resource allocation is recommended to be performed cooperatively based on ISAC. In contrast, the temporal resource assessment is recommended to be performed based upon MM4 whereby the incoming binary occupancy sequence is concluded by RSSI measurements or in case of autonomous medium access with a wideband spectrum sensing frontend. The sequence shall be extracted from the spectral resource assessment results. Finally, the temporal resource allocation is recommended to be performed in an autonomous reactive way in case of a combined spectrum sensing frontend, and in an autonomous proactive way in case of a dedicated spectrum sensing frontend to lower the latency.

9 Verwertbarkeit der Ergebnisse

Alle relevanten Ergebnisse wurden auf Konferenzen publiziert. Der Schlussbericht wird über die Homepage des Institut für industrielle Informationstechnik (inIT, www.init-owl.de) der Hochschule OWL verfügbar sein.

Webadresse des Projekts KOSYS:

<http://www.hs-owl.de/init/research/projects/b/filteroff/197/single.html>

10 Fortschritt des wissenschaftlichen und technischen Stands während der Laufzeit des Forschungsprojekts

Relevante veröffentlichte Ergebnisse anderer Forschungsgruppen wurden in die laufenden Forschungsarbeiten einbezogen. Insbesondere seien die folgenden Arbeiten genannt:

- Petri-Netze für die Simulation des Koexistenzverhaltens [33] und [34]: Dieser Ansatz ist alternativ zur ereignisgesteuerten Simulation zu sehen, die in diesem Vorhaben angewendet wurde. Der Ansatz über Petri-Netze bildet aufgrund einer idealen Funkkanal- und Koexistenzmodellierung reale industrielle Anwendungsszenarien nicht hinreichend ab.
- Kommunikations-Protokolle und Funkkanalsensorik bei kognitiven Funksystemen [49]: Die Ergebnisse dieser Veröffentlichung wurden berücksichtigt.
- Prädiktiver Kanalzugriff basierend auf Markov-Modellierung [52]: Dieser Ansatz wurde auch in diesem Projekt angewendet. Die Literaturstelle kann daher als Bestätigung der eigenen Arbeiten angesehen werden.

Darüber hinaus wurden die Forschungsansätze und erzielten Ergebnisse mit Wissenschaftlern anderer Forschungsgruppen auf Konferenzen diskutiert.

11 Veröffentlichung der Ergebnisse

Bisher erfolgten 7 Veröffentlichungen auf nationalen und internationalen Konferenzen. Außerdem erfolgte ein internationaler Workshop-Beitrag und eine Dissertation wurde veröffentlicht (Tabelle 3). Zahlreiche Reaktionen auf diese Veröffentlichungen haben das Forschungs- und Industrienetzwerk der Hochschule Ostwestfalen-Lippe deutlich ausgebaut.

Tabelle 3: Bisher erfolgte Publikationen

Y. Naderpour, D. Block, U. Meier: Evaluation of Deterministic Medium Access Based on a Cooperative Cognitive Radio Approach. The Fifth International Conference on Advances in Cognitive Radio - COCORA 2015, April 19 - 24, 2015, Barcelona, Spain
D. Block, U. Meier: A Novel Approach to Assess Wireless Coexistence. KommA 2014 – Jahreskolloquium Kommunikation in der Automation, Nov. 18, Lemgo
D. Block, Y. Naderpour, G. M. Shrestha, U. Meier: Performance Evaluation of Cognitive Wireless Medium Access Methods in Industrial Coexisting Environments. 19th IEEE Conference on Emerging Technologies and Factory Automation - ETFA 2014, Sept. 16 - 19, Barcelona, Spain
Kaleem Ahmad: Contributions to Improve Cognitive Strategies with Respect to Wireless Coexistence; Dissertation, Fakultät für Ingenieurwissenschaften, Universität Duisburg-Essen, 2013
D. Block, U. Meier: Coexistence Evaluation of Wireless Adaptive Medium Access Methods in Industrial Automation. KommA 2013 – Jahreskolloquium Kommunikation in der Automation, Nov. 13 - 14, Magdeburg
D. Block, U. Meier: Wireless Deterministic Medium Access: A Novel Concept Using Cognitive Radio (Best Paper Award). The Third International Conference on Advances in Cognitive Radio - COCORA 2013, April 21 - 26, 2013, Venice, Italy
D. Block: Medium Access Mechanism for Short Range Devices in Industrial Applications. In: Workshop CENELEC TC 65X, Brüssel, Belgien Oct 2012
K. Ahmad, U. Meier, S. Witte: Predictive Opportunistic Spectrum Access Using Markov Models. 17th IEEE Conference on Emerging Technologies and Factory Automation - ETFA 2012, Krakow, Poland
G. M. Shrestha, K. Ahmad, U. Meier: Statistical Analysis and Predictive Modeling of Industrial Wireless Coexisting Environments. 9th IEEE International Workshop on Factory Communication Systems - WFCS 2012, Lemgo/Detmold, Germany, May 2012

Über die Homepage des Instituts inIT (www.init-owl.de) stehen die Veröffentlichungen und der Abschlussbericht allen Interessierten zur Verfügung.

12 Anhang

12.1 Literaturverzeichnis

- [1] ZVEI: Koexistenz von Funksystemen in der Automatisierungstechnik, Erläuterungen zum zuverlässigen Parallelbetrieb von Funklösungen, ZVEI - Zentralverband Elektrotechnik und Elektronikindustrie e. V., 2008.
- [2] [Online]. Available: http://www.elektroniknet.de/kommunikation/news/article/30423/0/Droht_dem_24-GHz-Band_Ungemach/. [Zugriff am 13 11 2010].
- [3] J. Zhu, A. Waltho, X. Yang und X. Guo, „Multi-Radio Coexistence: Challenges and Opportunities,“ in *16th International Conference on Computer Communications and Networks*, 13-16 Aug. 2007.
- [4] K. Ahmad und U. Meier, „Coexistence optimization of wireless PAN automation systems,“ in *IEEE International Workshop on Factory Communication Systems*, 2008.
- [5] W. K. a. J. H. M. Konrad, „Coexistence Analysis of Bluetooth and Cellular UMTS in the 2500 - 2690 MHz Band,“ in *IEEE Wireless Communications and Networking Conference*, Las Vegas, NV, USA, 2006.
- [6] S. Suansook, S. Aramvith und P. Prapinmongkolkarn, „Comparative Performance Analysis of WiMAX and WLAN with WPAN Coexistence in UL Band,“ in *Intelligent Signal Processing and Communication Systems*, 2007.
- [7] U. Meier, S. Witte, K. Helmig, M. Hoeing, M. Schnueckel und H. Krause, „Performance Evaluation and Prediction of a Bluetooth Based Real-Time Sensor Actuator System in Harsh Industrial Environments,“ in *ETFA*, Greece, 2007.
- [8] Q. Pang und V. Leung, „Channel Clustering and Probabilistic Channel Visiting Techniques for WLAN Interference Mitigation in Bluetooth Devices,“ *IEEE Transactions on Electromagnetic Compatibility*, 2007.
- [9] T.-Y. Lin und Y.-C. Tseng, „Collision analysis for a multi-Bluetooth picocells environment,“ *IEEE Communications Letters*, Oct. 2003.
- [10] W. Yuan, X. Wang und J.-P. Linnartz, „A Coexistence Model of IEEE 802.15.4 and IEEE 802.11b/g,“ in *14th IEEE Symposium on Communications and Vehicular Technology in the Benelux*, 2007.
- [11] E. Toscano und L. Lo Bello, „Cross-channel interference in IEEE 802.15.4 networks,“ in *IEEE International Workshop on Factory Communication Systems*, 2008.
- [12] M. Herrera, A. Bonastre und J. Capella, „Performance Study of Non-beaconed and Beacon-Enabled Modes in IEEE 802.15.4 under Bluetooth Interference,“ in *The Second International Conference on Mobile Ubiquitous Computing, Systems, Services and*

Technologies, 2008.

- [13] D. Cassioli, R. Giuliano und F. Mazzenga, „Analysis of UWB system capacity in a realistic multipath environment with coexistence constraints,“ *IET Communications*, June 2007.
- [14] M. Hamalainen, e. al. und M. Latva-aho, „On the UWB system coexistence with GSM900, UMTS/WCDMA, and GPS,“ *IEEE Journal on Selected Areas in Communications*, Dec 2002.
- [15] A.-C. Hsu, D. Wei und C.-C. Kuo, „Coexistence Mechanism Using Dynamic Fragmentation for Interference Mitigation between Wi-Fi and Bluetooth,“ in *Military Communications Conference*, 2006.
- [16] K. Ohno und T. Ikegami, „Interference mitigation study for the coexistence of bi-phase UWB and multi-band OFDM,“ in *IEEE International Conference on UWB*, 2005.
- [17] P. He, Y. Lu, H. Zhang und J. Lu, „A pulse shaping method for UWB avoiding the frequency coexistence interference with WLAN,“ in *2nd International Conference on Mobile Technology, Applications and Systems*, 2005.
- [18] Y.-K. Kwok und M.-H. Chek, „Design and evaluation of coexistence mechanisms for Bluetooth and IEEE 802.11b systems,“ in *15th IEEE International Symposium on Personal, Indoor and Mobile Radio Communications*, 2004.
- [19] H.-U. Dehner, M. Linde, R. Moorfeld, H. Jakel, D. Burgkhardt, F. Jondral und A. Finger, „A low complex and efficient coexistence approach for non-coherent multiband impulse radio UWB,“ in *IEEE Sarnoff Symposium*, 2009.
- [20] L. Berlemann, C. Hoymann, G. Hiertz und B. Walke, „Unlicensed Operation of IEEE 802.16: Coexistence with 802.11(A) in Shared Frequency Bands,“ in *IEEE 17th International Symposium on Personal, Indoor and Mobile Radio Communications*, 2006.
- [21] Q. Pang und V. Leung, „Improved Channel Classification and Scheduling for Non-collaborative Bluetooth/ WLAN Coexistence,“ in *IEEE 63rd Vehicular Technology Conference*, 2006.
- [22] Q. Zhu und W. S. Wong, „Multi-Group Coexistence in License-Exempt Networks without Information Exchange,“ in *Cognitive Radio Oriented Wireless Networks and Communications*, 2007.
- [23] H.-S. Le und Q. Liang, „An Efficient Power Control Scheme for Cognitive Radios,“ in *IEEE Wireless Communications and Networking Conference*, 2007.
- [24] P. Tu, X. Huang und E. Dutkiewicz, „Adaptive Subband Selection in OFDM-Based Cognitive Radios for Better System Coexistence,“ in *3rd International Conference on Cognitive Radio Oriented Wireless Networks and Communications*, 2008.
- [25] K. Nolan, P. Sutton, L. Doyle, T. Rondeau, B. Le und C. Bostian, „Dynamic Spectrum

- Access and Coexistence Experiences Involving Two Independently Developed Cognitive Radio Testbeds," in *2nd IEEE International Symposium on New Frontiers in Dynamic Spectrum Access Networks*, 2007.
- [26] S. Geirhofer, L. Tong und B. Sadler, „Cognitive Medium Access: A Protocol for Enhancing Coexistence in WLAN Bands," in *IEEE Global Telecommunications Conference*, 2007.
- [27] Z. Wen, T. Luo, W. Xiang, S. Majhi und Y. Ma, „Autoregressive Spectrum Hole Prediction Model for Cognitive Radio Systems," in *IEEE International Conference on Communications Workshops*, 2008.
- [28] S. Geirhofer, L. Tong und B. Sadler, „Cognitive Medium Access: Constraining Interference Based on Experimental Models," *IEEE Journal on Selected Areas in Communications*, Jan 2008.
- [29] G. Bianchi, "Performance Analysis of the IEEE 802.11 Distributed Coordination Function," *Selected Areas in Communications, IEEE Journal*, pp. 535-547, 2000.
- [30] S. Y. Shin, W. H. Kwon and H. S. Park, "Interference Analysis of Coexistent Heterogenous Wireless Packet Networks based on Bit Error Rate," in *IEEE Global Telecommunications Conference GLOBECOM'07*, Washington, DC, USA, 2007.
- [31] S. Y. Shin, H. S. Park, S. Choi and W. H. Kwon, "Packet Error Rate Analysis of Zigbee under WLAN and Bluetooth Interferences," *IEEE Transactions on Wireless Communications*, pp. 2825-2830, 2007.
- [32] S. Y. Shin, J. S. Kang und H. S. Park, „Packet Error Rate Analysis of Zigbee under Interferences of Multiple Bluetooth Piconets," in *IEEE Vehicular Technology Conference VTC Spring 2009*, Barcelona, Spain, 2009.
- [33] A. Schmischar and L. Rauchhaupt, "Coexistence Analysis based on Petri Net Models," *IEEE Transactions on Industrial Informatics*, 2011.
- [34] A. Schimschar and M. Krätzig, "Assessment of LBT Systems using Petri Net Modelling," in *1st Conference on Embedded Systems, Computational Intelligence and Telematics in Control*, 2012.
- [35] S. Pollin, I. Tan, B. Hodge, C. Chun und A. Bahai, „Harmful Coexistence Between 802.15.4 and 802.11: A Measurement-based Study," in *Cognitive Radio Oriented Wireless Networks and Communications*, Singapore, 2008.
- [36] IEEE Standard for Information Technology – Local and Metropolitan Area Networks, *Specific Requirements – Part 15.4: Wireless Medium Access Control (MAC) and Physical Layer (PHY) Specifications for Low Rate Wireless Personal Area Networks (WPANs)*, 2006.
- [37] HART Communication Foundation, *WirelessHART Protocol Specification*, 2007.

- [38] IEEE Standard for Information Technology-Telecommunications and Information Exchange between Systems - Local and Metropolitan Area Networks, *Specific Requirements - Part 11: Wireless LAN Medium Access Control (MAC) and Physical Layer (PHY) Specifications*, 2007.
- [39] IEEE Standard for Information Technology - Telecommunications and Information Exchange Between Systems - Local and Metropolitan Area Networks, *Specific Requirements Part 11: Wireless LAN Medium Access Control (MAC) and Physical Layer (PHY) Specifications Amendment 8: Medium Access Control (MAC) Quality of Service Enhancements*, 2005.
- [40] Bluetooth SIG, *Bluetooth Core Specification v1. 2*, 2003.
- [41] IEEE Standard for Information technology - Local and metropolitan area networks, *Specific requirements- Part 15.1a: Wireless Medium Access Control (MAC) and Physical Layer (PHY) specifications for Wireless Personal Area Networks (WPAN)*, 2005.
- [42] P. Neufeld, U. Meier, L. Rauchhaupt and M. Krätzig, "A Unified Approach for the Assessment of Industrial Wireless Solutions," in *IEEE 16th Conference on Emerging Technologies & Factory Automation (ETFA)*, 2011.
- [43] K. Ahmad, U. Meier und S. Witte, „Predictive opportunistic spectrum access using Markov models,“ in *Conference on IEEE Emerging Technologies & Factory Automation (ETFA)*, Krakow, Poland, 2012.
- [44] G. M. Shrestha, K. Ahmad und U. Meier, „Statistical analysis and predictive modeling of industrial wireless coexisting environments,“ in *IEEE International Workshop on Factory Communication Systems (WFCS)*, Lemgo, Germany, 2012.
- [45] K. Ahmad, G. Shrestha und U. Meier, „Real-time issues of predictive modeling for industrial cognitive radios,“ in *IEEE International Conference on Industrial Informatics (INDIN)*, Caparica, Lisbon, 2011.
- [46] G. E. P. Box, G. M. Jenkins und G. C. Reinsel, *Time Series analysis: forecasting and control*, WILEY, 2008.
- [47] K. Ahmad, P. Ostfeld, U. Meier und H. Kwasnicka, „Exploitation of Multiple Hyperspace Dimensions to Realize Coexistence Optimized Wireless Automation Systems,“ *IEEE Transactions on Industrial Informatics*, Bd. 6, Nr. 4, pp. 758-766, 2010.
- [48] E. Hossain und V. K. Bhargava, „Cognitive Wireless Communication Network,“ in *Springer*, Vancouver, Canada, 2007.
- [49] J. Marinho und E. Monteiro, „Cognitive Radio: Survey on Communication Protocols, Spectrum Decision Issues, and Future Research Directions,“ in *Springer Science Business Media LLC*, New York, USA, 2011.
- [50] K. Ahmad, PhD Thesis: Contributions to Improve Cognitive Strategies with Respect to

Wireless Coexistence, Duisburg, Germany: University of Duisburg-Essen, 2013.

- [51] D. Block und U. Meier, „Wireless Deterministic Medium Access: A Novel Concept Using Cognitive Radio,“ in *COCORA 2013, The Third International Conference on Advances in Cognitive Radio*, Venice, Italy, 2013.
- [52] C. D. a. A. S. Alfa, „Predictive Channel Access in Cognitive Radio Networks based on Variable order Markov Models,“ in *GLOBECOM*, Houston, Texas, USA, 2011.
- [53] P. W. a. D. N. Vamsi Krishna Tumuluru, „A Neural Network Based Spectrum Prediction Scheme for Cognitive Radio,“ in *Communications (ICC), 2010 IEEE International* , Cape Town, South Africa, 2010.
- [54] I. A. Akbar und W. H. Tranter, „Dynamic spectrum allocation in cognitive radio using hidden markov models: Poisson distributed case,“ in *SoutheastCon*, Richmond, Virginia, USA, 2007.
- [55] S. Yarkan und H. Arslan, „Binary Time Series Approach to Spectrum Prediction for Cognitive Radios,“ in *Vehicular Technology Conference*, Baltimore, MD, USA, 2007.
- [56] H. Kim und K. Shin, „Efficient Discovery of Spectrum Opportunities with MAC layer Sensing in Cognitive Networks,“ in *IEEE transactions on mobile computing*, Trier, Germany, 2008.
- [57] R. C. Q. Zhe Chen, „Prediction of Channel State for Cognitive Radio Using Higher-Order Hidden Markov Model,“ in *IEEE SoutheastCon 2010* , Concord, NC, USA, 2010.
- [58] H. Su und X. Zhang, „Cross-Layer Based Opportunistic MAC Protocols for QoS Provisionings Over Cognitive Radio Wireless Networks,“ in *IEEE Journal on Selected Areas in Communications*, 2008.

12.2 Abkürzungsverzeichnis

AFH	Adaptive Frequency Hopping
ARP	Address Resolution Protocol
BER	Bitfehlerwahrscheinlichkeit
CCA	Clear Channel Assessment
CSMA/CA	Carrier Sense Multiple Access with Collision Avoidance
CTS	Clear To Send
DAA	Detect and Avoid
DAE	Differential Algebraic Equation
DAR	Detect and Reduce
DAS	Detect and Suppress
DUT	Device Under Test
FFT	Fast Fourier Transform
FHSS	Frequency Hopping Spectrum Spreading
FSM	Finite State Machine
GTS	Guaranteed Time Slots
IA	Industrielle Automatisierungstechnik
ISM	Industrial, Scientific and Medical
IX	Interfer

MAC	Media Access Control Layer
MAM	Medium Access Method
MF	Membership Function (fuzzy logic)
MO	Medium Occupancy
NETW	Networking Layer
ODE	Ordinary Differential Equation
PHY	Physical Layer
PLR	Packet Loss Rate
PDS	Power Density Spectrum
RBW	Resolution Bandwidth
RTS	Request To Send
RX	Receiver
SINR	Signal-to-Interference-plus-Noise Ratio
SUT	System Under Test
SWT	Standard Wireless Technology
TDMA	Time Division Multiple Access
TNR	Specificity (True Negative Rate)
TPR	Sensitivity (True Positive Rate)
TT	Transmission Time

TX	Transmitter
----	-------------

VSG	Vector Signal Generator
-----	-------------------------

WLAN	Wireless Local Area Network basierend auf IEEE 802.11
------	---

WPAN	Wireless Personal Area Network
------	--------------------------------
